

Response to Editor and Reviewers

[1] We thank the editor and two reviewers for their comments and suggestions. We have made several revisions accordingly, which we explain below. The line numbers refer to the annotated m/s version with changes marked.

Response to Editor

I have read the very detailed comments from both reviewers, as well as the detailed responses you have provided to each of these comments. It strikes me that the points raised primarily require clarification, as they stem from confusion on the part of the reviewer.

You have made several clear comments on how you propose to update the manuscript to help clarify the points raised. Mostly your suggestions are clear. However, in several cases you leave it as reply to the comment. I would encourage you to consider adding one or two words/phrases to help clarify the confusion. This is useful for those readers who may be equally confused but are not inclined to go through all the interactive comments and replies (which I would suspect to be the majority).

[2] Agreed. We have made textual changes to pre-empt similar questions or issues wherever we saw an opportunity, as explained in our responses below.

Response to Reviewer #1

I think the comment on WR3A models is different should be addressed in the manuscript, as you are not clear if you will do this. It is I think important to point out that the structure of the model is important in being able to apply the approach presented, which precludes other perhaps simpler water balance type models.

[3] Agreed, we have added such a sentence (see response [11]).

On the flow diagram. This may indeed be useful, but as it primarily has the purpose to clarify, you may consider including it in the supplementary material.

[4] We have made and included such a flow diagram. In revising we initially included it in the supplement, but it seemed a bit out of place there and so we moved it into the main text. We would gladly take advice, however.

Response to Reviewer #2

I agree that it is not necessarily beneficial to the readability of the manuscript if all the details on model formulations are included in the main manuscript. In fact this may even be detrimental. The suggestion to include these in the supplementary material is I think a good one, but I would also restrict that to not overburden these, as references are indeed given to more complete descriptions. I trust the authors can assess what additional information is useful here. The authors should of course clearly refer the reader to the supplementary material as appropriate in the main manuscript to ensure the link can be made where it is required. Perhaps that would also have helped this reviewer find the relevant detail.

[5] In response to the reviewer comments we moved a description of the forcing and downscaling to the main text. With that gone, it appeared that the information that was previously in the Appendix could instead be provided in the main text without too much additional text, so we did that. We provided some more textual detail on the process descriptions. Including all energy balance equations would have to be added as a supplement, which did not seem to make much sense as the model equations are already documented online, as the editor points out.

It may be worth considering including the figure providing comparison against FLUXNET values in the supplementary material, in support of the comments in the main text. However, I would include in the main text a comment that you do not consider these as true validation I presume due to the issue of representation. This is commented on but maybe useful to add that additional sentence to clarify. Also, what is mean by N=16-168. Is this a typo?

[6] Agreed, we have taken the editor's advice and included more detail in the supplement, and also added an explicit statement along the lines suggested. We agreed the $N=16-168$ was confusing and changed it. It was not a typo as such, $N=16$ was for the study of Yebra, and $N=168$ for our unpublished analysis, which is now in the supplement (in revising this number increased to $N=169$ due to an additional site)

On the discussion on "before reaching ocean", and the need for better maps of closed basins. I would add to this that the reaching of the ocean is often also influence by evaporation (and the increase of evaporation due to irrigation). So while the DEM may indicate the river reaches the ocean, water in the river in fact does not. You could consider that not reaching the ocean is due to either being a closed basin or due to anthropogenic influences.

[7] Agreed, see responses [51]-[53]

I would like to suggest the authors update the manuscript based on the comments and the suggestions they have made in response. In that update please clearly outline the changes.

[8] Thank you. Below we outline the changes made. We also provide a copy of the m/s with the changes marked for the convenience of editor and reviewers.

Response to Reviewer #1

[9] We thank the reviewer for their comments and are glad that they enjoyed the m/s. We are also grateful for the editorial corrections and suggestions. Below we address the issues raised.

"The authors mention how all kind of modelling efforts will not produce independent and accurate estimates of irrigation water demand, but after the reading the objective I can only conclude that they will themselves do modelling as well. I think it would be good to refocus the introduction and state that models can have a valuable contribution but have their limitations and highlight how the authors would like to resolve these limitations."

[10] It is certainly true that our approach requires a model to assimilate the satellite observations into, and it is also true that additional assumptions are needed to translate water use estimates to irrigation water demand. We meant to emphasise that our method differs from existing methods in that it does not require mapping of the area irrigated or the extent of wetlands to estimate secondary evaporation. In revising, we added:

"Such an approach still involves modelling and the assumptions inherent to it, but the greater use of observations should mitigate against errors arising from the modelling." (l. 94-95)

"I do not fully understand why this model is different from the other global water balance models out there. They authors should do a better job to highlight this, to emphasize why this model is better suited for this excursive than others"

[11] The overall approach is different from existing models in that secondary evaporation is constrained by the satellite observations, rather than the result of simulation. If the reviewer refers to the W3RA model used in assimilation, then we believe a similar approach could be applied to other models, provided they have a coupled water and energy balance model and provided they are extended for data assimilation in the way described. We added:

"The W3RA model used here it not the only suitable modelling framework for the approach described. A similar method could be applied with other local or global models. The main requirements are that the model has a coupled water and energy balance model that simulates LST, and that it is amenable to data assimilation." (l. 168-171)

"The quality of the forcing data is really low, how do the authors think this will impact the simulations and consequently the evaporation estimates?"

[12] This question does not have a simple answer. The model takes several forcing data as input, the evaporation estimates are not equally sensitive to all of them, and the quality of forcing data also varies spatially and temporally

(seasonally as well as at longer time scales due to advances in satellite sensors). Hence it is impossible to give a quantitative answer to the question, but with regards to evaporation (only), one observed issue is that of heterogeneous biases in air temperature in regions with strong relief. Fortunately, secondary losses occur mostly in areas with low relief (see original text). To emphasise this more, we have added:

“A systematic bias in the global estimates of governing variables (radiation, air temperature and humidity, wind speed) are likely to be less problematic than spatially variable bias in these low-relief areas.” (l. 596-598)

“Line 184-185 and Figure 1, I have the strong feeling that the model is biased in its estimates of E. Therefore, this would violate the basic assumption of a normal distribution with a mean of 0 around the observations. In addition, the authors cut-off the E' updates, which is in my opinion another violation of the EnKF. I feel the others should make sure that the model is bias free before implementing a DA technique like the EnKF. Otherwise, they can show the global biases to convince the reader that this is only the case for Figure 1, but I have to strong suspicion that it is also a problem for other regions (as for most models). I think the authors should address this large limitation in their discussion or somewhere else in the manuscript.”

[13] Does the reviewer mean the model is biased in the absence of secondary evaporation (i.e. in drylands)? We do not have evidence for that. We have evaluated the (“offline” or background) model against evaporation rates reported by the global Fluxnet network for non-irrigated environments and did not find any bias, which is not surprising given the model was partly trained on those same data. We added the details of the evaluation, previously described as “unpublished”, in a new supplement.

[14] The reviewer suggests showing global biases, but there are no global ET observations (other than Fluxnet) to calculate those from. However, we do compare with estimates from other models and find that ours are well within that range (see discussion in original text).

[15] We did not use EnKF but nudging based on energy balance model inversion.

[16] The reviewer is correct that we did cut off the E' updates. This was necessary to maintain internal physical consistency, but it is true that it may have introduced bias, particularly if the real E was consistently higher than the available energy, for example due to biases in meteorological forcing data. In revising the m/s, we have added:

“Values of the updated $\lambda E'$ were constrained to positive values below or equal to potential evaporation E_0 , and therefore any gross underestimation of E_0 by the model due to errors in meteorological forcing data would have resulted in an underestimation of the true evaporation rate.” (l. 588-591)

“The manuscript could significantly benefit from a flowchart describing the full updating, calibration, nudging and assimilation procedure. Which variable are subject to what and where and how? The manuscript is difficult to follow without.”

[17] Thank you for the suggestion. Data assimilation procedures are often difficult and tedious to explain but we have added a flow diagram to attempt to illustrate it better, and added the following explanation:

The methodology of our experiment includes two mostly separate components (Figure 1). The assimilation component integrates various MODIS products into the global hydrological model to estimate the dryland water balance and secondary evaporation. Subsequently, in an offline analysis the estimates of secondary evaporation were combined with mapping of irrigated crops to estimate a minimum irrigation requirement. Below follow details on the model, the data assimilation procedure, estimation of irrigation water use, and the different ways in which the results were evaluated. Details on the data used in the analysis can be found in the supplement to this article.

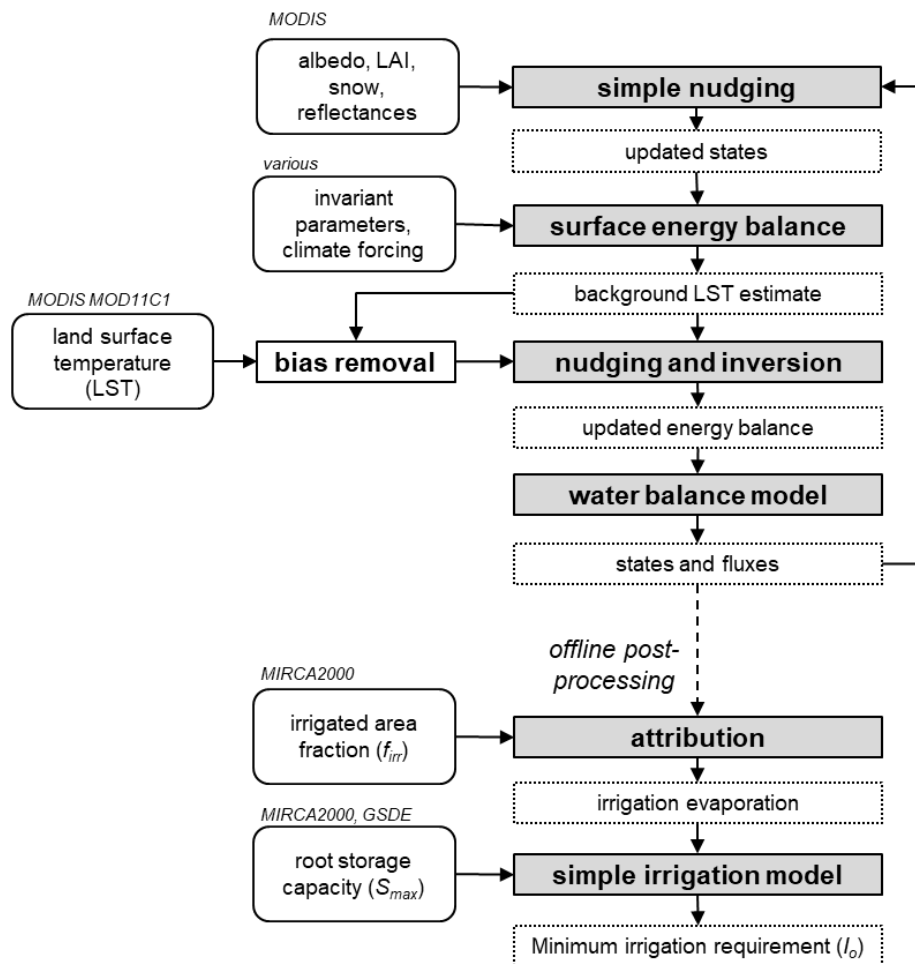


Figure 1. Illustration showing the processing steps and data used in each step. Acronyms relate to input data that are described in the text.

(l. 112-121)

“Line 253-254 Why is the increase in the estimation evaporation not from missing model processes? Incorrect vegetation parameterization or something else. This assumption is vital for the manuscript and is not really supported by argument on the model’s quality to estimate evaporation in general. Has the model been validated against independent evaporation estimates?”

[18] This was discussed in the original m/s (l. 558-567 in the annotated revised m/s): the assimilation of satellite vegetation observations goes some way to address errors in vegetation parameterization. However, the (necessary) assumption that the assimilation increment is due to irrigation has uncertainty associated with it (but only if) most of a grid cell is occupied by non-irrigated land. Hence also the recommendation that our approach should work better at higher resolution, which we hope to pursue.

[19] Regards validation: see response [13].

“In addition, to the previous comment, the authors have not mention other forms of water use. I see no inclusion of domestic or industrial water use in the model nor in the estimates? Maybe these abstractions cause the errors in water basin closures.”

[20] Domestic and industrial water use are not considered because these are typically non-consumptive uses (i.e., the water is returned to the environment after use). Possibly the main exception to this would be irrigation in urban landscapes, which the irrigation mapping does not capture well or at all. If those uses lead to surface cooling then the LST data assimilation will still have increased E estimates and so they are implicitly accounted for. In practice,

consumptive urban or industrial water uses are unlikely to have a meaningful impact on the water balance of large basins. We added:

“Domestic and industrial withdrawals are not considered here as a large fraction of these withdrawals is not evaporated but returned to the environment.” (l. 391-393)

“Line 129-134 are the calibrated parameter spatially consistent or are they really tuned to the individual basins?”

[21] Neither, they vary spatially as a function of climate aridity and land cover using predictive relationships derived from model calibration to evaporation, soil moisture and streamflow from a very large number of sites and small and unregulated catchments, respectively. This was described in the original m/s, but we added a bit more detail in l. 155-162.

“Line 134-135 Does the model have any lateral flow simulations of groundwater or surface water?”

[22] No, only grid-based routing.

“Line 150 a nudging factor of 0.99 is rather high, does this mean that the model is almost always wrong?”

[23] Poor at predicting highly dynamic surface water extent, one could say, yes. (Like all global models, to the best of our knowledge.) We added:

“(reflecting the low skill in the model to accurately predict surface water extent at 0.05° resolution)” (l. 184-185)

“Line 156-159 what is the spatial resolution of the Tair forcing, since it is very important for the LST simulations”

[24] We agree that correct Tair is important, although the median bias correction step reduces most of the systematic difference, which we would argue is one of the novel aspects of our approach and one reason for its apparent success. These details were in the appendix, but we agree that they are probably important enough to be explained in the main text. Therefore we added:

“Monthly precipitation and air temperature climatology data at 30” from the WorldClim dataset (Hijmans et al., 2005) were resampled to 0.05° and 0.25°; subsequently, the ratio and difference, respectively, between the data at the finer and coarser resolution were applied to the forcing data.” (l. 145-150)

“Line 177 15degree, does this mean that the LST is spatially average over a 1500 by 1500km area???”

[25] A 15x15° region is indeed about that size at lower latitudes. Note that this does not imply that LST is assumed homogenous across the area. This calculation is to remove the mean bias between daytime LST and time-of-overpass LST. We added *“to remove systematic bias”* (l. 213)

“Line 508-510 the true error can also be larger. . . It is not said that it will be smaller due to the representativeness error.”

[26] In theory, yes, although given the rather large sample such a statistical accident would be unlikely. Nonetheless we removed this statement, for the more important reason that the relatively large uncertainty in Fluxnet energy balance terms means that they do not provide a very reliable assessment of possible bias in our model estimates (see new supplement).

“Line 581-583 As far as I understand most other models use sub-grid parameterization, which would allow for a partial coverage of the grid cell by irrigation areas. This statement is therefore potentially incorrect and should be removed to avoid misinforming the reader”

[27] We respectfully disagree. The MIRCA2000 mapping suggests the grid cell is 100% equipped for irrigation. To our knowledge the published models assume that the entire equipped area is irrigated so the statement holds. Of course that assumption could be changed for another.

“Line 619-623 I feel the units are incorrect, I guess the first estimates should be $75.5 \cdot 10^{12} \text{ km}^3 \text{ y}^{-1}$ (as well as for the other estimates from this study, which are now 1000 times lower than other studies)

[28] The units are correct. We could have written $75,500 \text{ km}^3 \text{ y}^{-1}$ but felt using base units (m) was more appropriate, as neither unit is easily imagined.

Response to Reviewer 2

[29] We thank the reviewer for their positive and constructive comments. Below we respond to the issues raised.

“First of all, I find the manuscript a bit unbalanced in terms of contents. There is a lot of focus on methods and equations (esp. for irrigation), but relatively a few figures for results. This makes the manuscript very tedious to read with a lot of text and information. At the same time, some information that are critical to assess the results are either missing or in the appendix. For example, forcings and their spatial disaggregation, model formulations of LE and H, etc.”

[30] We are sorry the m/s was tedious to read. We appreciate that the technical detail of the modelling and data assimilation can be a bit tedious, which is why we tried to minimise that aspect in the body text by transferring some of the material to the appendix and referring to existing studies where possible. We have added 2 figures: one illustrating the workflow, and one with some new analysis suggested by the reviewer. We hope this has made the m/s less tedious.

[31] The referee also asks for additional material to be included and we therefore made some additions. We have added further details on “forcings and their spatial disaggregation” in the main text (see response [24]). The “model formulations of LE and H” were described in the methods section. The energy balance equation is the main model component of relevance here, but it is in essence a conventional implementation of the Penman-Monteith equation, which is well-known and the detail of the implementation is readily available online already. We did some additional text to explaining the approach however:

“The surface energy and water balance is simulated using the Penman-Monteith model. The evaporative fluxes from transpiration, unsaturated soil, saturated soil and surface water are simulated subject to the overall constraint of potential evaporation E_0 within the same Penman-Monteith framework. Wet canopy evaporation is simulated outside this constraint, for reasons described in Van Dijk et al. (2015), using a dynamic-canopy version of the event-based Gash model (Van Dijk and Bruijnzeel, 2001; Wallace et al., 2013).” (l. 133-138)

“Definition of the secondary evaporation: There is no description on how groundwater’s contribution to LE/ET is a secondary source. In an idealistic theoretical situation, the capillary flux from groundwater will replenish soil moisture (at some point when the soil moisture is drying up), which would eventually increase LE. It is not clear if the model considers such capillary flux processes explicitly. I am curious about what fraction of ‘other’ sources is actually coming from groundwater-soil-LE pathway, and not groundwater-baseflow-surface water-LE pathway. The first one may have a critical influence on vegetation and carbon cycle processes.”

[32] The model does consider capillary fluxes, but in the offline model those are ultimately constrained by longer-term local rainfall, and therefore do not constitute secondary evaporation (i.e., it is derived from locally recharged, unconfined groundwater rather than lateral groundwater inflows). As our study demonstrates, data assimilation helps to estimate secondary evaporation from non-local water sources, but does not directly attribute it to a water source – that requires ancillary data. In some cases, the secondary evaporation may be from irrigation with water pumped from confined aquifers (which bypasses the capillary rise pathway). In other cases, it is possible that secondary evaporation is inferred, e.g. because rainfall is underestimated, capillary rise or deep root water uptake is more important than predicted by the background model (e.g., because the vegetation is more deeply rooted or groundwater is closer to the surface than assumed). There is obviously much more to be done to understand the global water balance in full detail. Our data provide a means of prioritising regions where there appears to be

hydrological behaviour that is not easily explained by the background model, and therefore is worthy of further investigation. To make clear that capillary rise is possible within the model, we added the following words:

“[The soil column is conceptualised as a three-layer unsaturated zone overlaying an unconfined groundwater store], from which capillary rise can occur.” (l. 130-131)

“Assimilation of LST into model: In the assimilation of LST into model, the basic assumption is that the model-simulated partitioning of the energy fluxes (H and E) are correct. The corrections or ‘nudges’ for LST are back-calculated from the modelled H, and these are propagated through spatial patterns of observed LST. But, there is no explanation of how ‘background’ H and LE are calculated in the model. Perhaps, these may be inferred from previous papers/reports on the model (?), but they are so critical for this study and results presented herein, they deserve to be in this manuscript.”

[33] The basic assumption is actually not that the partitioning of H and LE is correct, but rather, that the estimated total available energy ($A=H+LE$) is correct. Data assimilation may change the estimate of H, and through that $LE=A-H$. To make this clear we added:

“A fundamental assumption in this approach is that the partitioning between λE and H can be improved with information on LST, but that the estimate of available energy A is correct.” (l. 224-226)

[34] The background H and LE are estimated using the conventional Penman-Monteith approach. We have added new details on that in the model description section (see [31]).

“One information that is imperative is whether the parameters of the modelled LE and H were optimized or not. If not, are the used parameter values are reasonable for a global-scale application?”

[35] The most important parameter overall, surface conductance, was predicted from satellite-observed surface reflectances following Yebra et al. (2013) and tuned using a large data base of evaporation measurements (FLUXNET). Another important parameter, vegetation height (affecting aerodynamic conductance) was derived from remote sensing by Simard et al. (2011). We have added a few additional words to hopefully make the approach clearer:

“Global datasets were also used to parameterise the distribution of different land surface types (Bicheron et al., 2008) and the properties of vegetation (Simard et al., 2011), soil (Shangguan et al., 2014), and aquifers (Gleeson et al., 2014; Beck et al., 2015).” (l. 150-152)

and

“[Five model parameters that were both relatively uncertain and influential were calibrated and regionalised] by climate and land cover type class, [using large global data sets of site measurements evaporation and near-surface soil moisture, and a global dataset of catchment streamflow records (the parameters represent proportional adjustments to initial estimates of, respectively, maximum canopy conductance, relative canopy rainfall evaporation rate, soil evaporation, saturated soil conductivity, and soil conductivity decay with depth).]” (l. 1487-153)

“Related to the above point, validation for model simulated LE and H is not shown or discussed. There are references to a previous study or an unpublished work but the findings of this study also warrant a section on evaluations at the global scale. I am aware that observed global ET and H data are not available, but a comparison with either FLUXNET observations (for sites) or other satellite-based ET products can provide a valuable benchmark.”

[36] In response, we have summarised the result of the unpublished evaluation and included it as a new supplement. We believe putting it in the main text would be misleading readers into thinking it constitutes an assessment of the performance in estimating secondary evaporation, which it does not: the vast majority of flux towers are in environments without secondary evaporation. This was also the reason we initially did not think it a good idea to include it, but we can see that a reader might want to see anything that is referred to and that “unpublished”

therefore might not cut it. As the supplement makes clear, the flux tower observations also suffer from the energy balance closure problem which makes evaluation more ambiguous.

[37] A comparison with other global ET products was discussed in the original m/s.

“Estimation of irrigation water use: Assumption of rooting depth: The parameter s_{max} is dependent on the assumed rooting depth. The manuscript would benefit from a discussion on how these parameters vary globally, and to what extent do this variation affects the estimation of secondary evaporation from irrigated area.”

[38] We follow the published methodology of Siebert and Döll (2010). The assumptions made here do not affect the estimation of secondary evaporation. They do affect is the calculated irrigation efficiency and therefore the estimate of irrigation water use. This is a perhaps subtle, but important distinction. We added additional text in to places to make sure this is clear:

“The assimilation component integrates various MODIS products into the global hydrological model to estimate the dryland water balance and secondary evaporation. Subsequently, in an offline analysis the estimates of secondary evaporation were combined with mapping of irrigated crops to estimate a minimum irrigation requirement.” (l. 112-116)

and

“The estimation of I_0 was done after, and entirely separate from, the data assimilation process, and therefore what follows had no bearing on the estimation of secondary evaporation.” (l. 267-269)

“Evaluation against discharge observations: In my subjective judgment, the improvement in the basins with discharge < 300 mm/y is mostly driven by Paraná because it has discharge with the largest magnitude. In reality, the river basins with large irrigation water withdrawal/use are also equipped with dams and are not of run-of-river type (with no reservoir). The secondary evaporation from these ‘dammed’ rivers also comprise of evaporation from reservoirs. So, in my opinion, it would be helpful to include the information of reservoir volume (e.g., from Grand database) in the analysis or the figure. This is important because the water evaporated from the reservoirs might actually be significant, especially because the irrigation requirement/use from this study is much lower than previous estimates.”

[39] Actually, it is also due to the improved water budget for closed basins (dots on the vertical axis) and several other basins (e.g., Indus). Our methodology does use remotely sensed water extent, and that would include reservoir surface area, so evaporation from reservoir surfaces is included in the estimates.

“Comparison with previous estimates: The manuscript addresses the minimum irrigation water requirement, which I understood as the actual gross irrigation water use (gross because it has both bare soil evaporation in irrigated areas+transpiration by crops). In most previous modeling studies, difference between PET and ET is used to calculate irrigation water requirement (and withdrawal). Current manuscript rightly points that there are several limitation to ET from irrigated areas. Despite that, it would make sense to compare the difference between PET and ET (Priestley Taylor is already used in the current study) with the bias of I_0 against withdrawal.”

[40] Unfortunately we did not grasp the analysis the reviewer proposes. In the original m/s, we did compare I_0 to reported withdrawals in Fig 5 and l. 435-449, and this does provide some useful insights, discussed in l. 561-599. We could compare irrigation area ET to PET (as done for example in Fig. 2e in the revised m/s) but are not sure how to summarise such a comparison globally or what it would demonstrate.

“Forcing variables: The results of this study are extremely dependent on the biases in the WFD forcing data as well as the spatial patterns of HYDROCLIM data. It is not clear from the current analysis if the biases in secondary evaporation are related to WFD magnitude (over a half degree grid) or the spatial patterns of HYDROCLIM (over 0.05 deg grids).”

[41] The term ‘extremely’ is subjective, but given the Penman-Monteith energy balance approach used, the evaporation estimates will depend on the meteorological forcing data, as does any method to estimate evaporation.

We used the relative spatial patterns in the high-resolution, station-based WorldClim dataset to downscale air temperature only (see [24]). Because we only assimilated satellite LST in areas with modest relief, we do not expect that the downscaling will have had much effect on secondary evaporation estimates. We also suspect that biases in air temperature in the WFD forcing data may in fact be less important than uncertainties in the radiation balance, wind speed, and perhaps specific humidity. Because we have not separately investigated or quantified these uncertainty sources, we prefer not to speculate and leave such interpretations to the reader. Nevertheless, in the revised m/s we acknowledge that uncertainties in the forcing data could have an impact on the results (l. 558).

“Temporal variation of secondary evaporation: I would have really learnt a lot on what is driving the secondary evaporation if there was a discussion on temporal variation of secondary evaporation at the global scale. This would provide insights on whether the secondary evaporation increases in wet season (for e.g., in water bodies such as wetlands and river channels because the surface area becomes larger) or in dry season in which the groundwater access by plant can be expected to be maximum.”

[42] We thank the reviewer for the suggestion and have performed some additional analysis. We have added the following results:

“There is a pronounced seasonal cycle in secondary evaporation at global scale (Figure 11). The rate of secondary evaporation is more than two times higher in northern summer than in northern winter. This is primarily due to the greater rate of evaporation from the many surface water bodies in formerly glaciated regions, including the American Great Lakes, as well as a higher rate of evaporation from the Caspian Sea. By contrast, secondary evaporation in regions located wholly or partially in the southern hemisphere show a much less pronounced seasonal cycle and a greater influence of water availability. Averaged over time, each of the regions considered makes a similarly sized contribution to secondary evaporation globally (10–24%) with the exception of Antarctica (0.4%).”

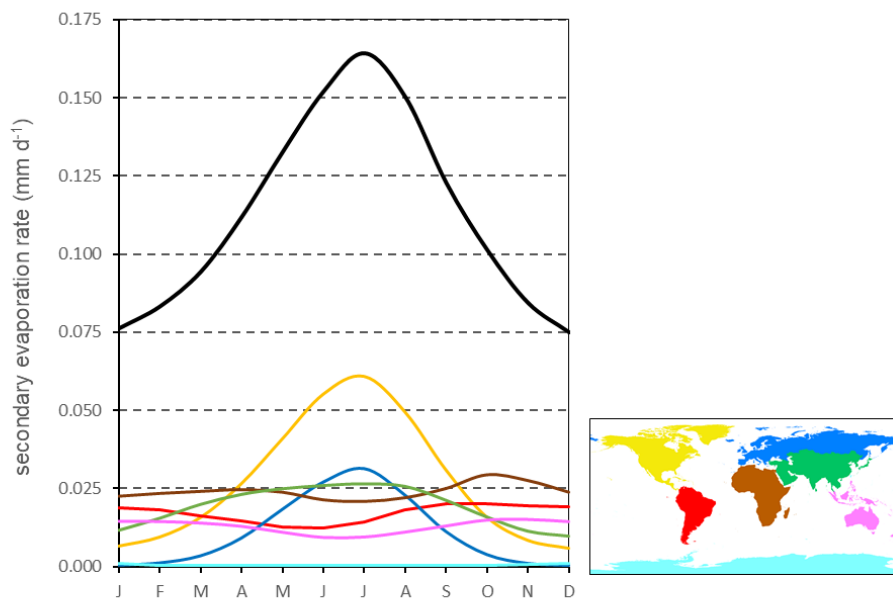


Figure 11. Average (2001–2012) seasonal cycle of secondary evaporation at global scale (black line) and the contribution from different regions (colours corresponding to the map). All rates are expressed in mm d-1 for the global land area.” (l. 535-543)

We are not sure whether these findings are very relevant from a global water cycle or climate system perspective, but if the reviewer finds them interesting then perhaps they satisfy a certain curiosity in other readers as well. The main driver of the seasonality is ultimately due to the legacy of glaciation, and so we have added the following to the discussion:

“There is a strong seasonal cycle in secondary evaporation at global scale, driven by evaporation from extensive surface water bodies in formerly glaciated regions in the northern hemisphere. This illustrates the profound impact that glaciation has had on regional landscape hydrology, and its influence at global scale.” (l. 696-699).

“Evaporation larger than precipitation in southern Africa and Yucatan: The discussion focuses on the biases in the precipitation. If total E (primary + secondary) were correct, the signal should appear in the water storage changes. In that case, GRACE satellite measurements should show a declining terrestrial water storage. A comparison on loss of storage in the study period and the total E – P would provide a great motivation for future studies on what are driving such changes. Essentially, this would already help in refining the potential causes of the negative water budget.”

[43] Again we thank the reviewer for the suggestion. Some knowledge of GRACE based trends was on our mind in interpreting the results, but we did not make this explicit. A previous GRACE model-data assimilation study some of the authors were involved in inferred that water storage did decrease slightly over the Yucatan peninsula between 2003 and 2012 but increased quite strongly in southern Africa. Neither trend was predicted by an ensemble of hydrological models (particularly not for the African case), which led us to suspect deficiencies in the rainfall estimates driving those models. We expanded the discussion as follows.

“We analysed global water cycle reanalysis data that integrated GRACE gravity observations in an earlier study (Van Dijk et al., 2014) for a largely overlapping period (2003–2012) to test this. For the African Southern Interior, the reanalysis demonstrated a clear increasing trend in subsurface storage (+12.3 mm y⁻¹) that was not reproduced by an ensemble of models (+2.0 mm y⁻¹). This suggests that the global precipitation estimates used by models were indeed too low for this period, as also concluded by Van Dijk et al. (2014). For the Yucatan peninsula, a slight storage decrease (-3.3 mm y⁻¹) was inferred from the reanalysis, whereas the model ensemble suggested a slight increase (2.7 mm y⁻¹). This does not suggest any underestimation of precipitation. A net use of groundwater does appear plausible in this case, though likely not enough to explain the secondary evaporation rates estimated here” (l. 622-632)

Editorial Comments:

“Line 1: In my opinion, ‘estimates’ should be replaced by ‘simulations’. Essentially, the results are dependent on hydrological model simulations.”

[44] We respectfully disagree. Satellite observations were assimilated to make the results less dependent on model simulations.

“Line 232: i=1,26 can be replaced by just 26.”

[45] We used this notation to make the meaning of i in A_i in the same sentence clear.

“Line 259: There is no description for what P_g is. I assumed that it is precipitation for the grid cell.”

[46] Apologies, this should have read P_{irr}. We corrected this.

“Figures 6-9: I recommend using the same color maps and scales in these figures. It is a bit confusing because the same color ‘blue’ means a different value in different figures.”

[47] Thank you, we made this change.

“Table 1: Just curious that observed discharge in Nile is 0. Fascinating that no water from such large river basin reaches the ocean.”

[48] Agreed.

“Line 534: can have affected → can affect or could have affected”

[49] Agreed, thank you.

“Line 621: wrong units: km³/yr → m³/yr

[50] Agreed, thank you.

“Line 671-673: → Before reaching the ocean is misleading because a fraction of the open water evaporation is from rivers which do not drain to ocean (e.g., inland lakes).

[51] For clarification, we changed this to:

“Around 16% of globally generated water resources evaporate before reaching the oceans or from closed basins, enhancing total terrestrial evaporation by 8.8%.” (l. 752-754)

[52] We do not consider the statement to have been misleading, however. Our phrasing was chosen for pragmatic reasons, although there is also a conceptual argument. The pragmatic reason was that, in identifying closed basins, we found it challenging to separate “truly” closed basins from basins that DEM analysis suggested were closed but which actually did appear to have an overflow according to independent reports. Surprisingly, it appears that there is no reliable global map of closed basins, and it took background research to identify the basins shown in Fig. 3. There were many other basins that the DEM suggested were closed but where we were not able to confirm that, meaning we ultimately did not identify all closed basins and therefore cannot make the distinction between secondary evaporation from (all) closed basins and all ocean reaching rivers.

[53] The conceptual reason is that the referee’s argument can in fact be turned around: those rivers in ‘closed basins’ do not drain to the ocean because evaporation is so high. The difference between closed and ocean-draining basins is a threshold (lake) level, and some basins currently switch between these states depending on the difference between rainfall and evaporation, many others did in the past. We do accept that there are closed basins that would require a very large increase in rainfall indeed (or decrease in evaporation) to top the overflow threshold and start draining to the ocean, but it does mean that there is no fundamental difference between ‘closed’ and ‘open’ basins.

[54] We do believe that a map of all (currently) closed basins would be a valuable information source for water balance studies, and are currently looking into producing one using DEM data of higher accuracy and resolution, but early indications are that it requires intensive quality control. If it had existed, we would have made the distinction.

“Line 674-678: Does the groundwater include baseflow-river-ET and groundwater capillary flux-soil moisture-ET? I am not sure if the second process can be categorized as the secondary evaporation.”

[55] We are not entirely sure how to interpret this question. In case it answers the question, we did add:

“[The soil column is conceptualised as a three-layer unsaturated zone overlaying an unconfined groundwater store], from which capillary rise can occur.” (l. 130-131)

Thus, the primary evaporation estimates by the model do include the effect of capillary rise. However, if the primary evaporation estimates are too low data assimilation increases those estimates, and the difference will be (perhaps partly or wholly incorrectly) ascribed to secondary evaporation from lateral inflows. We discussed this in l. 501-504 of the original m/s.

1 **Global 5-km resolution estimates of secondary evaporation including irrigation**
2 **through satellite data assimilation**

3

4 Albert I.J.M. van Dijk¹, Jaap Schellekens^{2,3}, Marta Yebra¹, Hylke E. Beck⁴, Luigi J.
5 Renzullo¹, Albrecht Weerts^{2,5}, Gennadii Donchyts²

6

7 ¹Fenner School of Environment & Society, Australian National University, Canberra, ACT, Australia

8 ²Deltares, Delft, The Netherlands

9 ³Vandersat B.V., Haarlem, The Netherlands

10 ⁴Princeton University, Princeton, NJ, USA

11 ⁵Wageningen University & Research, Wageningen, The Netherlands

12

13

14 **Abstract**

15 A portion of globally generated surface and groundwater resources evaporates from wetlands, water
16 bodies and irrigated areas. This secondary evaporation of ‘blue’ water directly affects the remaining
17 water resources available for ecosystems and human use. At the global scale, a lack of detailed water
18 balance studies and direct observations limits our understanding of the magnitude and spatial and
19 temporal distribution of secondary evaporation. Here, we propose a methodology to assimilate
20 satellite-derived information into the landscape hydrological model W3 at an unprecedented 0.05° or
21 c. 5 km resolution globally. The assimilated data are all derived from MODIS observations, including
22 surface water extent, surface albedo, vegetation cover, leaf area index, canopy conductance, and land
23 surface temperature (LST). The information from these products is imparted on the model in a simple
24 but efficient manner, through a combination of direct insertion of surface water extent, evaporation
25 flux adjustment based on LST, and parameter nudging for the other observations. The resulting water
26 balance estimates were evaluated against river basin discharge records and the water balance of closed
27 basins and demonstrably improved water balance estimates compared to ignoring secondary
28 evaporation (e.g., bias improved from +38 mm/d to +2 mm/d). The evaporation estimates derived
29 from assimilation were combined with global mapping of irrigation crops to derive a minimum
30 estimate of irrigation water requirements (I_0), representative of optimal irrigation efficiency. Our I_0
31 estimates were lower than published country-level estimates of irrigation water use produced by
32 alternative estimation methods, for reasons that are discussed. We estimate that 16% of globally
33 generated water resources evaporate before reaching the oceans, enhancing total terrestrial
34 evaporation by $6.1 \cdot 10^{12} \text{ m}^3 \text{ y}^{-1}$ or 8.8%. Of this volume, 5% is evaporated from irrigation areas, 58%
35 from terrestrial water bodies and 37% from other surfaces. Model-data assimilation at even higher
36 spatial resolutions can achieve a further reduction in uncertainty but will require more accurate and
37 detailed mapping of surface water dynamics and areas equipped for irrigation.

38

39 **Introduction**

40 The generation of surface and groundwater resources is commonly conceptualised one-dimensionally
41 as the net difference between precipitation, evaporation (including transpiration) and soil storage
42 change. However, some part of the generated ‘blue’ water (Falkenmark and Rockström, 2004)
43 subsequently inundates floodplains, accumulates in wetlands and freshwater bodies, or is extracted for
44 irrigation. A fraction of that water will evaporate in this second instance. This ‘secondary
45 evaporation’ directly reduces the remaining blue water resources available for ecosystems and
46 economic uses downstream but also increases the use of water by terrestrial ecosystems before
47 discharging into the oceans. At the global scale, our understanding of the magnitude and
48 spatiotemporal distribution of secondary evaporation is limited by a lack of detailed water balance
49 studies and direct observations. Until recently, land surface models ignore lateral water transport and
50 secondary evaporation altogether or provide a rudimentary description. This is understandable, given
51 the complexity and computational challenge in simulating the lateral redistribution and secondary
52 evaporation of water at the global scale. However, it is increasingly clear that the lateral redistribution
53 of water cannot be ignored in global water resources analyses (Oki and Kanae, 2006; Alcamo et al.,
54 2003), carbon cycle analysis (Melton et al., 2013) and regional and global climate studies (e.g., Thiery
55 et al., 2017).

56 Even approximate numbers on the importance of secondary evaporation in the global water cycle are
57 not available. Oki and Kanae (2006) derived global bulk estimates of gross evaporation from lakes,
58 wetlands and irrigation (combined $10.1 \cdot 10^{12} \text{ m}^3 \text{ y}^{-1}$) but their estimate was based on modelling only
59 and included both primary and secondary evaporation. There have been some studies estimating
60 irrigation water requirements at the global scale (Döll and Siebert, 2002; Wada et al., 2014; Siebert
61 and Döll, 2010) but these studies were based on idealised modelling, did not attempt to separate
62 between primary and secondary evaporation, and did not consider other sources of secondary
63 evaporation.

64 There have been attempts to use satellite observations to estimate the importance of secondary
65 evaporation at a regional scale. For example, Doody et al. (2017) used MODIS-based evaporation
66 estimates (Guerschman et al., 2009) over Australia to delineate areas receiving lateral inflows. They
67 used ancillary data to attribute these to surface water inundation, irrigation, and groundwater-
68 dependent ecosystems, respectively. At the global scale, Wang-Erlandsson et al. (2016) used satellite-
69 based ET estimates from several sources to infer rooting depth, which provided some insights into the
70 spatial distribution of surface- and groundwater dependent ecosystems.

71 Historically, three contrasting approaches have been followed to estimate evaporation: water balance
72 modelling; inference from land surface temperature (LST) remote sensing; and estimation based on
73 vegetation remote sensing. All three approaches rely on meteorological data and effectively involve a
74 land surface model of some description, albeit of variable complexity. Hybrids between the three
75 approaches have also been developed over time to mitigate respective weaknesses (Glenn et al.,

76 2011). For example, dynamic simulation of the soil water balance can provide a valuable constraint on
77 satellite-based evaporation estimates in water-limited environments; provided precipitation is the only
78 source of water for evaporation, and accurate precipitation estimates are available (Glenn et al., 2011;
79 Miralles et al., 2016). However, where there are additional sources of water or unexpected soil
80 moisture dynamics, applying this constraint can degrade evaporation estimates.

81 Beyond dynamic hydrological models, evaporation products based more closely on vegetation remote
82 sensing implicitly account for the effect of lateral water redistribution on transpiration, but often do
83 not account for open water evaporation (Yebra et al., 2013; Zhang et al., 2016), with exceptions
84 (Guerschman et al., 2009; Miralles et al., 2016). Satellite-observed LST has a direct, physical
85 connection to the surface heat balance, and through the overall surface water and energy balance can
86 provide a constraint on evaporation estimates. Several techniques have been developed to infer
87 evaporation from LST, and many successful applications at local scale have been documented (Kalma
88 et al., 2008). Over larger areas, the application of LST-based methods is complicated by the need for
89 time-of-overpass estimates of radiation components, air temperature, and aerodynamic conductance
90 (Kalma et al., 2008; Van Niel et al., 2011). There are promising developments that can overcome
91 some of these challenges (Anderson et al., 2016), although they are yet to be fully evaluated.

92 Arguably, the most promising approach to evaporation estimation is to combine water balance
93 modelling, LST remote sensing, and vegetation remote sensing within a model-data fusion
94 framework. Such an approach still involves modelling and the assumptions inherent to it, but the
95 greater use of observations should mitigate against errors arising from the modelling. This prospect
96 motivated the present study.

97 *Aim*

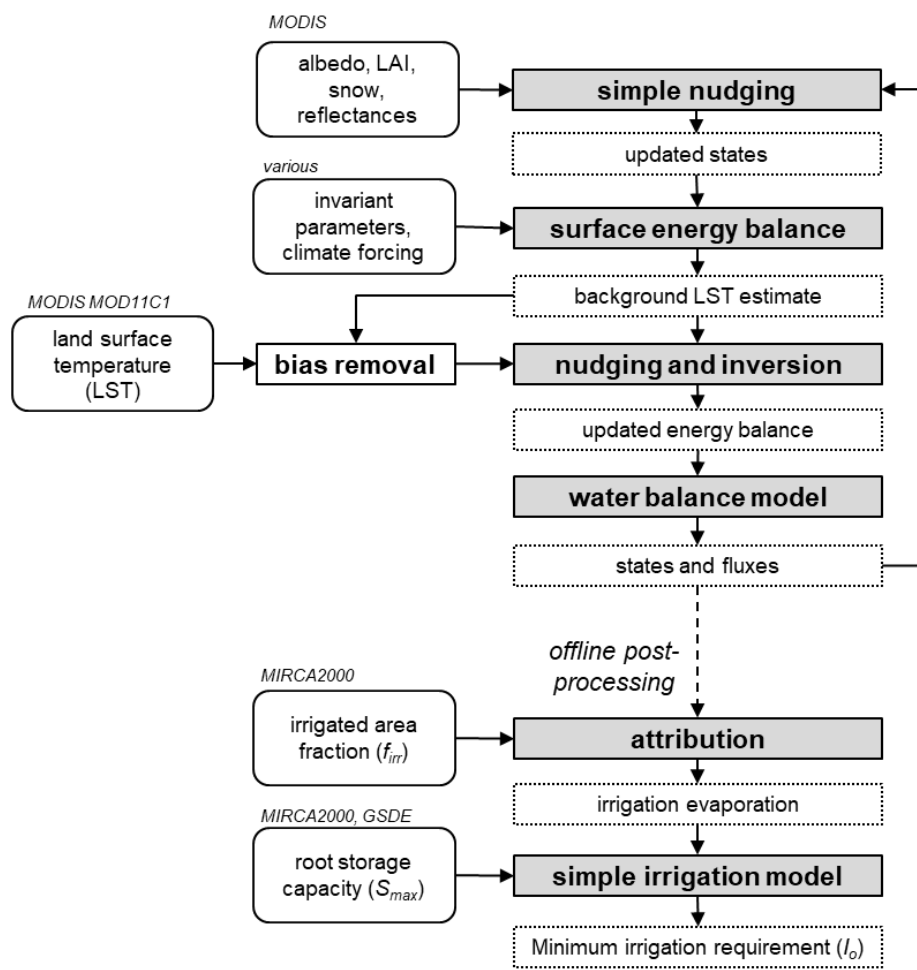
98 Our objective was to develop a methodology to assimilate optical and thermal observations by the
99 MODIS satellite instruments into a 0.05° resolution global hydrological model to estimate
100 evaporation and to evaluate the quality and quantitative accuracy of the resulting estimates as much as
101 possible. Based on the resulting estimates, we wished to answer the following questions:

- 102 • What is the magnitude of secondary evaporation of surface and groundwater resources in the
103 global and regional water cycle?
- 104 • What is the magnitude of irrigation evaporation and how does it relate to total agricultural water
105 withdrawals?
- 106 • What are the contributions of secondary evaporation from irrigation, permanent water bodies,
107 ephemeral water bodies, and other surfaces?
- 108 • Is secondary evaporation likely to have a noticeable impact on the global carbon cycle and
109 climate system?

110

111 **Materials and Methods**

112 The methodology of our experiment includes two mostly separate components (Figure 1). The
 113 assimilation component integrates various MODIS products into the global hydrological model to
 114 estimate the dryland water balance and secondary evaporation. Subsequently, in an offline analysis
 115 the estimates of secondary evaporation were combined with mapping of irrigated crops to estimate a
 116 minimum irrigation requirement. Below follow details on the model, the data assimilation procedure,
 117 estimation of irrigation water use, and the different ways in which the results were evaluated. Details
 118 on the data used in the analysis can be found in the supplement to this article.



119
 120 Figure 1. Illustration showing the processing steps and data used in each step. Acronyms relate to input data that
 121 are described in the text.

122
 123 *Global water balance model description*

124 The World-Wide Water model (W3) version 2 is an evolution of the AWRA-L and W3RA group of
 125 models. The AWRA-L model is used operationally for water balance estimation across Australia at
 126 0.05° resolution by the Bureau of Meteorology. An overview of the operational AWRA-L model

127 (version 5) can be found in Frost et al. (2016b), with details on the scientific basis in Van Dijk (2010).
128 Very briefly, the model operates at daily time step and is grid-based. Each cell is conceptualised to
129 represent several parallel small, identical catchments. The soil column is conceptualised as a three-
130 layer unsaturated zone overlaying an unconfined groundwater store, from which capillary rise can
131 occur. The unsaturated soil water balance and corresponding water and energy fluxes can be
132 simulated separately for hydrological response units (HRUs) that each occupy a fraction of the grid
133 cell. The surface energy and water balance is simulated using the Penman-Monteith model. The
134 evaporative fluxes from transpiration, unsaturated soil, saturated soil and surface water are simulated
135 subject to the overall constraint of potential evaporation E_0 within the same Penman-Monteith
136 framework. Wet canopy evaporation is simulated outside this constraint, for reasons described in Van
137 Dijk et al. (2015), using a dynamic-canopy version of the event-based Gash model (Van Dijk and
138 Bruijnzeel, 2001; Wallace et al., 2013). Sub-grid parameterisations are applied to simulate the area
139 fractions with surface water, groundwater saturation and root water access to groundwater
140 dynamically, based on the hypsometric curves (i.e., the cumulative distribution function of elevation)
141 for each grid cell (Peeters et al., 2013).

142 The W3 (version 2) model is a global implementation of AWRA-L (version 5) at the same 0.05°
143 resolution. Important differences are as follows (~~details in Appendix A~~). Separate HRUs were not
144 considered, however, the water balance of permanent water bodies is calculated separately. Global
145 gridded climate time series and surface, vegetation and soil parameterisation data were used. In brief,
146 MSWEP v1.1 (Beck et al., 2017) precipitation estimates and other meteorological data from the
147 WFDEI v1 dataset (Weedon et al., 2014). Monthly precipitation and air temperature climatology data
148 at $30''$ from the WorldClim dataset (Hijmans et al., 2005) were resampled to 0.05° and 0.25° ;
149 subsequently, the ratio and difference, respectively, between the data at the finer and coarser
150 resolution were applied to the forcing data. Global datasets were also used to parameterise the
151 distribution of different land surface types (Bicheron et al., 2008) and the properties of vegetation
152 (Simard et al., 2011), soil (Shangguan et al., 2014), and aquifers (Gleeson et al., 2014; Beck et al.,
153 2015). We used the cumulative distribution function of Height Above Nearest Drainage (HAND;
154 Nobre et al., 2015) for each grid cell instead of hypsometric curves, which we derived from high-
155 resolution global digital elevation models.

156 Five model parameters that were both relatively uncertain and influential were calibrated and
157 regionalised by climate and land cover type class, using large global data sets of site measurements
158 evaporation and near-surface soil moisture, and a global dataset of catchment streamflow records (the
159 parameters represent proportional adjustments to initial estimates of, respectively, maximum canopy
160 conductance, relative canopy rainfall evaporation rate, soil evaporation, saturated soil conductivity,
161 and soil conductivity decay with depth). Differences less relevant here include the addition of a snow
162 water balance model with parameters from Beck et al. (2016) and grid-based river routing using a
163 flow direction based on HydroSheds (Lehner et al., 2008) where available and HYDRO 1k elsewhere.

164 A range of W3-simulated water and energy balance terms has been made publicly available as part of
165 ‘Tier-2’ of the earth2Observe project (Schellekens et al., 2017). The AWRA-L and W3 models have
166 received extensive evaluation, demonstrating realistic estimates of evaporation, soil moisture, deep
167 drainage, streamflow and total water storage (e.g., for more recent implementations, Tian et al., 2017;
168 Frost et al., 2016a; Beck et al., 2016; Holgate et al., 2016).

169 The W3RA model used here is not the only suitable modelling framework for the approach described.
170 A similar method could be applied with other local or global models. The main requirements are that
171 the model has a coupled water and energy balance model that simulates LST, and that it is amenable
172 to data assimilation.

173 *Data assimilation*

174 All data assimilated here were derived from NASA’s Moderate Resolution Imaging
175 Spectroradiometer (MODIS) instruments. The data included albedo, reflectance, leaf area index (LAI)
176 and LST (~~details in Appendix A~~). We followed the following steps, except for LST. First, the MODIS
177 band reflectances ([product MCD43C4.005](#)) were used to estimate vegetation cover fraction and
178 canopy conductance following Yebra et al. (2015; 2013); surface water extent was estimated
179 following Van Dijk et al. (2016); and MODIS albedo ([MCD43C3.005](#)), snow cover fraction
180 ([MCD43C4.005](#)) and [the MODIS GLASS LAI products-product \(Xiao et al., 2014\)](#) were used in their
181 original form. Next, seven model states were updated using a simple nudging scheme. For each state,
182 the observation and model error estimates were based on an assessment of the noise in the
183 observational data, the expected dynamic rate of change, and the expected skill of the model. The
184 resulting ‘gain’ factors (i.e. the relative weight of observations) varied from 0.5 for LAI and snow
185 fraction to 0.99 for surface water fraction (reflecting the low skill in the model to accurately predict
186 surface water extent at 0.05° resolution). The updated states were also used dynamically to update six
187 related parameters of diagnostic model equations, including a parameter relating vegetation cover
188 fraction to canopy conductance, another relating vegetation cover to LAI, and four parameters relating
189 surface state to albedo.

190 The approach to assimilate LST observations was different. In this case, the dynamic model was run
191 one timestep forward to produce a background estimate of the surface energy balance and evaporation
192 flux. The corresponding average daytime LST (T_s , K) was estimated from the average daytime
193 sensible heat flux (H , W m^{-2}) as

$$194 \quad T_s = T_a + \frac{H}{\rho_a c_p g_a} \quad (1)$$

195 where T_a is air temperature (K), ρ_a air density (kg m^{-3}), c_p specific heat capacity ($\text{J kg}^{-1} \text{K}^{-1}$), and $g_a(u)$
196 aerodynamic conductance (mm s^{-1}). The latter is a function of wind speed scaled by the wind speed
197 measurement and vegetation heights, respectively, following Thom (1975).

198 Poor characterisation of spatial gradients in radiative exposure, air temperature, and wind speed in
199 areas with relief can cause a poor relationship between observed and modelled LST (Kalma et al.,
200 2008). Fortunately, secondary evaporation primarily occurs in regions with low relief. Therefore, data
201 assimilation was only attempted for areas with an average slope less than 3% (as calculated from the
202 higher resolution DEM; ~~Appendix A~~). This threshold was empirically found to include a large
203 majority of observed surface water inundation and mapped irrigation areas.

204 A second challenge relates to the inconsistency between the observation time-of-overpass LST and
205 model-predicted mean daytime LST. We assumed that time-of-overpass and mean daytime LST will
206 have different spatial averages, but share a near-identical spatial pattern of deviations from the spatial
207 averages. This assumption also helps to remove systematic bias, which is the largest source of error in
208 MODIS LST estimates ~~used here (MOD11C1.006; Wan, 2015)~~. Previous assessments report errors in
209 MODIS that are within 0.7 K under conducive atmospheric conditions but can increase to 3 or 4 K
210 due to errors in atmospheric correction that tend to cause similar level of bias over a larger area (Wan
211 et al., 2004; Wan, 2008; Wan and Li, 2008; Hulley et al., 2012).

212 In the assimilation step, ~~first~~ the median observed and modelled LST were calculated for all low-relief
213 grid cells within a spatial window of 15° latitude and longitude and subtracted from the respective
214 gridded LST values ~~to remove systematic bias~~. Subsequently, we calculated the difference between
215 resulting observed and modelled LST values. The calculated difference was reduced by up to 1 K to
216 conservatively allow for uncertainty in the assumptions and errors in the observations. Next, the
217 model LST was updated with the remaining difference towards the MODIS-observed LST. An
218 updated latent heat flux ($\lambda E'$ in W m^{-2} ; the prime indicating the updated variable) can be calculated
219 from ~~the an inverted version of the~~ energy balance ~~equation~~ as

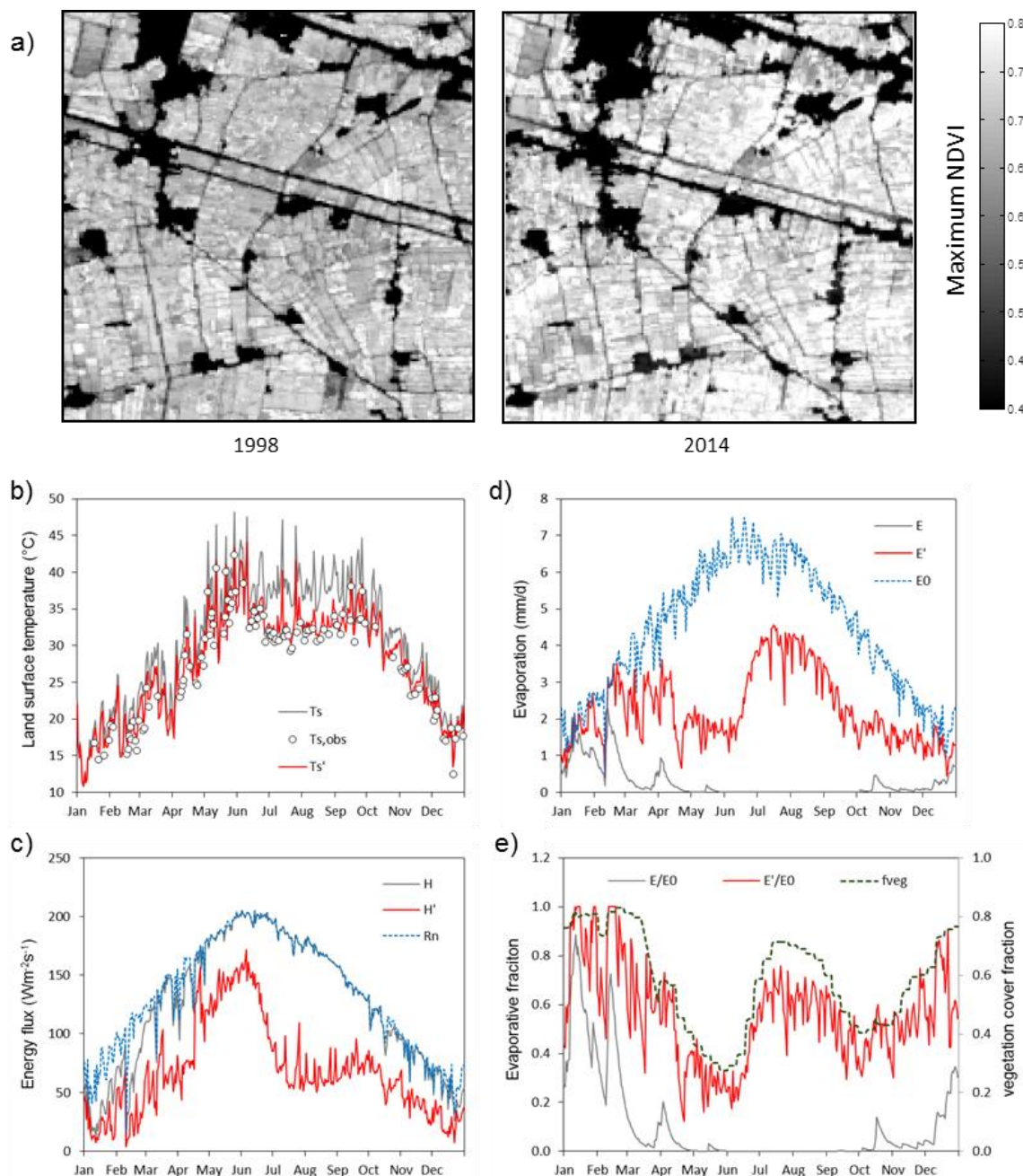
$$220 \quad \lambda E' = A - H' = A - \rho_a c_p g_a (T_s' - T_a) \quad (2)$$

221 where A is available energy (W m^{-2}). To ensure physical consistency within the model context, $\lambda E'$
222 was constrained to positive values below or equal to ~~potential evaporation E_o , calculated following~~
223 ~~Penman-Monteith theory (details in Van Dijk, 2010)~~. Temporal consistency was ensured by recording
224 the ratio $\lambda E'/\lambda E$ and using it to adjust simulated λE for subsequent days until a new LST observation
225 was available. Finally, E was calculated through division by the latent heat of vaporisation λ . ~~A~~
226 ~~fundamental assumption in this approach is that the partitioning between λE and H can be improved~~
227 ~~with information on LST, but that the estimate of available energy A is correct.~~

228 To illustrate the data assimilation, time series of observations and model results for one 0.05° grid cell
229 in the Nile delta in Egypt are shown in ~~Figure 1~~ ~~Figure 2~~. This grid cell was chosen because it
230 represents one of comparatively few grid cells worldwide deemed to be 100% equipped for irrigation
231 in global mapping (although annual maximum NDVI derived from Landsat suggests that only 80–
232 81% of the area is in fact irrigated; ~~Figure 1~~ ~~Figure 2~~a). The processing steps are illustrated by a
233 comparison of observed, background and analysis LST estimates for the year 2002 (~~Figure 1~~ ~~Figure~~

234 | 2b), and the resulting sensible heat flux (Figure 2c) and daily evaporation (Figure 2d).
 235 | Corresponding temporal patterns in the evaporative fraction (E/E_0) show that data assimilation
 236 | brings the temporal pattern of evaporative fraction in close agreement with satellite-observed
 237 | vegetation cover fraction (Figure 2e), which provides as a largely independent consistency
 238 | test.

239



240

241 | [Figure 2](#). Illustration of method to assimilation MODIS land surface temperature observations. Data
 242 | shown are for 2002, for 0.05° grid cell in the Nile River delta, Egypt (centred 31.075°N, 30.325°E). (a)

243 | *Maximum normalised difference vegetation index (NDVI) derived from Landsat imagery provided by Google*

244 Earth Engine, suggesting that effectively 81% and 80% of the grid cell was cropped in 1998 and 2014,
245 respectively. (b) *Land surface temperature*: background (T_s , grey line), observed ($T_{s,obs}$, circles) and analysis
246 (T_s' , red line) estimates for the grid cell with average bias across the 15° window removed. (c) *Sensible heat*
247 *flux*: background (H , grey) and analysis (H' , red) estimates along with net radiation (R_n , blue). (d) *Evaporation*:
248 background (E , grey) and analysis (E' , red) estimates along with potential evaporation (E_0 , blue). (e)
249 *Evaporative fraction*: background (E/E_0 , grey) and analysis (E'/E_0 , red) along with vegetation cover fraction
250 derived from MODIS NDVI (f_{veg} , green).

251 *Irrigation water use estimation*

252 For irrigated areas, the long-term average difference between precipitation and total evaporation
253 derived from data assimilation provides an estimate of the importance of additional water inputs.
254 However, it cannot be interpreted directly as an estimate of irrigation water requirements, much less
255 as an estimate of water withdrawals. This is because precipitation and crop water requirements are
256 both unevenly distributed in time, and there is limited water storage capacity in the crop root zone.
257 Additional water is lost from the root zone through drainage and runoff, which will need to be
258 compensated by additional irrigation inputs. This field-level irrigation inefficiency does not
259 necessarily change the long-term net water balance: provided total precipitation and evaporation do
260 not change, the additional inputs will equal the additional runoff and drainage. However, such
261 inefficiencies do need to be accounted for when estimating the total amount of irrigation water
262 required (Siebert and Döll, 2010).

263 Estimating total field-level irrigation water requirements is sensitive to assumptions about the
264 capacity for added water to remain stored in the root zone irrigation and about strategies (e.g.,
265 pursuing a stable low or high soil moisture or paddy water level, suboptimal or soil moisture deficit
266 irrigation, flood irrigation or partial drip irrigation, and so on). Here, we estimated a minimum field-
267 level irrigation requirement (I_0 in mm), which can be taken as a conservatively low estimate of
268 irrigation that represents highly efficient irrigation practices. The estimation of I_0 was done after, and
269 entirely separate from, the data assimilation process, and therefore what follows had no bearing on the
270 estimation of secondary evaporation.

271 We used global mapping by crop type to estimate I_0 using a plausible range of published assumptions
272 about water storage capacity. It was assumed that irrigation is just sufficient to replenish lost water
273 without any direct drainage or runoff losses; that is, losses only occur when precipitation exceeds
274 available storage capacity. Following Siebert and Döll (2010), we estimate the available root zone
275 storage capacity (S_{max} in mm) ~~capacity~~ for $i=1..26$ irrigated crop types based on the estimated
276 harvested area (A_i in ha) of each as contained in the MIRCA2000 dataset (Portmann et al., 2010).
277 These numbers are combined with assumed rooting depth (z_i) and the allowable fraction of depletion
278 of available soil water p_i (Allen et al., 1998) for each crop type as proposed by Siebert and Döll
279 (2010). The plant available water content (θ_a) was estimated using global soil property data
280 (Shangguan et al., 2014; ~~see Appendix A~~), calculated as the difference between θ at field capacity and

281 permanent wilting point, assumed to correspond to water potential values of -3.3 and -150 m,
 282 respectively. In formula:

$$283 \quad S_{max} = \frac{\sum A_i z_i p_i}{\sum A_i} \theta_a f_{irr} \quad (3)$$

284 where f_{irr} is the fraction of the grid cell area that is equipped for irrigation (Portmann et al., 2010).
 285 This method produced a global average root zone storage of 51 mm per unit of irrigated land, with
 286 90% of values between 10–85 mm, with values depending primarily on the value of z_i .

287 Because we have observation-based estimates of evaporation, we do not simulate the influence of soil
 288 water status on evaporation, but instead, propagate a simple water balance model forced with
 289 evaporation estimates. In words, the change in soil moisture storage from one day (S_t) to the next
 290 (S_{t+1}) is the net result of gross rainfall onto the irrigated area (P_{irr}), evaporation from the irrigated area
 291 (E_{irr}), the minimum irrigation water application required (I_0) and drainage (D), with storage and
 292 cumulative fluxes (all in mm):

$$293 \quad S_{t+1} = S_t + P_{irr} - E_{irr} + I_0 - D \quad (4a)$$

294 Partial rainfall (P_{irr}) is proportional to the irrigation fraction and grid cell rainfall (P):

$$295 \quad P_{irr} = f_{irr} P \quad (4b)$$

296 It is assumed that any increase in the estimate of evaporation ($E' - E$) from data assimilation is due to
 297 irrigation, where this occurs, and therefore E_{irr} is given by:

$$298 \quad E_{irr} = f_{irr} E + (E' - E) \quad (4c)$$

299 Any soil water additions more than maximum storage capacity (S_{max}) are assumed to become
 300 drainage, and irrigation is assumed to be just enough to prevent $S < 0$:

$$301 \quad I_0 = \max(E_t - P_{irr} - S_t, 0) \quad (4d)$$

$$302 \quad D = \max(S_t + P_{irr} - E_t - S_{max}, 0) \quad (4e)$$

303 Rainfall interception losses are included in E . Surface runoff and residual drainage are assumed
 304 negligible when $S < S_{max}$. This is an important simplification, but consistent with the definition of a
 305 minimum irrigation requirement estimate that reflects optimal efficiency. The daily water balance
 306 model was evaluated with an initial state of $S = S_{max}$ and propagated from 2000–2014. The first year
 307 was not used in subsequent calculations to allow for artefacts from the initial state chosen.

308 *Evaluation of basin water balance*

309 One test of the accuracy of secondary evaporation estimates is to evaluate whether their inclusion in
 310 the basin water balance improves agreement with observations. The difference between E' derived
 311 from data assimilation and the background estimate E is interpreted to be derived from lateral inflows:

312
$$E_{lat} = E' - E \quad (5a)$$

313 For any basin, the total net amount of discharge from the basin (Q_n) is the result of the gross amount
 314 of streamflow generated in all tributaries (Q_g) minus secondary evaporation of flows downstream
 315 (E_{lat}) and the change in storage derived from those flows (ΔS_{lat}):

316
$$Q_n = Q_g - E_{lat} - \Delta S_{lat} \quad (5b)$$

317 Natural storage variations in soil and groundwater and river channel storage are explicitly simulated
 318 by the model and not included in ΔS_{lat} . Storage changes in other surface water bodies (e.g., lakes and
 319 reservoirs), river-groundwater exchanges, and induced soil or groundwater storage changes directly
 320 related to inundation or irrigation (including pumping) would affect ΔS_{lat} . It is assumed here that the
 321 magnitude of ΔS_{lat} is negligible compared to the other terms if fluxes are averaged over the period
 322 2001–2014. This needs to be considered when interpreting results for individual basins.

323 We used discharge data for large basins to evaluate whether our estimates of E_{lat} improved the overall
 324 agreement between modelled and observed Q_n . The river discharge data used were drawn from the
 325 global database of end-of-river discharge records compiled by Dai et al. (2009). This includes data for
 326 925 rivers worldwide. Out of these, we considered only basins for which more than five years of data
 327 were available during 1995–2014. This longer period was adopted because few basins had sufficient
 328 measurements after 2000. To avoid errors arising from differences in the delineation of basins, we
 329 rejected basins with a catchment area less than 100,000 km² and those with a reported drainage area
 330 that was more than 25% different from the DEM-derived basin area at the river mouth. For the
 331 remaining 38 large basins, the temporal and area-average discharge was calculated and compared to
 332 the modelled Q_n and Q_g (all in mm y⁻¹).

333 Closed or endorheic basins represent a special case where $Q_n=0$ and can also be used to construct a
 334 water balance. The 0.05° flow direction grid was used to delineate all internally draining basins
 335 located between 72°N and 60°S (further poleward the DEM is affected by land ice). Adjoining
 336 endorheic basins were merged into contiguous regions to avoid incorrect basin delineation. From the
 337 resulting regions, all those with a surface area greater than 50,000 km² were extracted, resulting in 13
 338 contiguous regions. For these regions, Eq. (5b) was evaluated and compared to the expected $Q_n=0$.

339 The LST data assimilation changes evaporation without adjusting other water balance terms and
 340 hence does not conserve mass balance. In both open and closed basins, this can produce a positive or
 341 negative Q_n from Eq. (5b). A difference between estimated and observed Q_n can occur for any of four
 342 reasons: Q_g is underestimated, E_{lat} overestimated, ΔS_{lat} is non-negligible, or (for discharging basins
 343 only) recorded Q_n is in error.

344 *Evaluation of apparent irrigation water use*

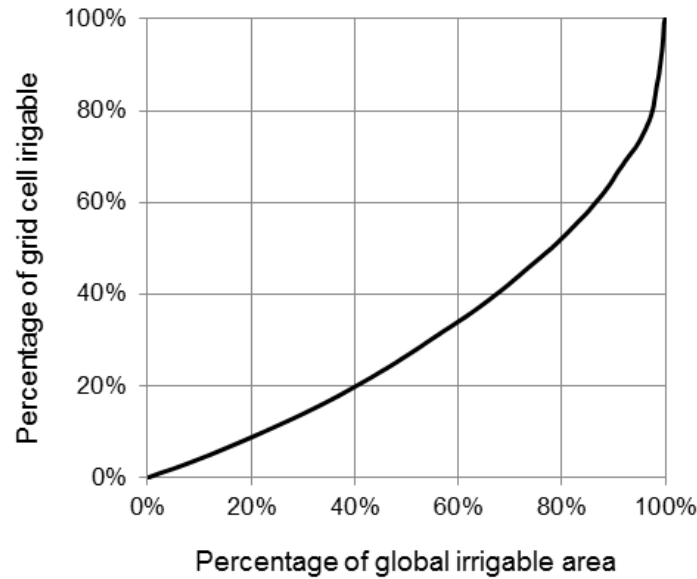
345 Evaluating estimates of secondary evaporation due to irrigation is challenging. Direct observations of
 346 evaporation from irrigated land are not widely available, represent point observations, and include

347 primary evaporation. At basin or country level, estimates of irrigation water use can be categorised as
348 'bottom-up' or 'top-down' estimates. Bottom-up estimates require scaling of estimated crop water use
349 to field-level irrigation requirements. Top-down estimates involve estimating large-scale withdrawals
350 (e.g., by differencing of discharge measurements along a river reach or measured bulk diversions) and
351 accounting for "project" or scheme losses along the distribution network (Bos and Nugteren, 1990).
352 Both approaches have large uncertainties but provide estimates of the order of magnitude of irrigation
353 water use.

354 Bottom-up estimates of irrigation water use at the global scale and for individual countries are
355 available from previous studies (Siebert et al., 2010; Wada et al., 2014; Siebert and Döll, 2010). They
356 involve soil-vegetation water balance modelling. Similar to the approach used here, these methods
357 require assumptions about root zone storage capacity, the rate of drainage of water from the root zone,
358 the permissible range of root zone soil moisture, and the efficiency of irrigation. Unlike the approach
359 used here, they furthermore require assumptions about evaporation, usually following FAO's crop
360 factor approach (Allen et al., 1998) to model crop water use. The resulting one-dimensional irrigation
361 water requirement estimates are subsequently extrapolated spatially using mapping of areas equipped
362 for irrigation (e.g., Portmann et al., 2010), using assumptions about the number of crop rotations and
363 the area factually irrigated. Each of these assumptions introduces errors and uncertainties.
364 Nonetheless, a comparison with these studies should provide insight into the method developed here.

365 An important source of uncertainty in our estimation of large-scale I_0 is due to the diffuse spatial
366 distribution of irrigated areas, which is further amplified in current mapping products. The mapping of
367 areas equipped for irrigation contained in the MIRCA2000 dataset (Portmann et al., 2010) was done at
368 0.08° grid resolution and linearly interpolated to 0.05° resolution in this study. Even at this high
369 resolution, a large proportion of total irrigable land occupies only a small fraction of a grid cell
370 ([Figure 2](#)[Figure 3](#)).

371



372

373 | **Figure 2****Figure 3.** Cumulative distribution curve or quantile plot describing the degree to which the global
 374 irrigable area is concentrated. It shows that, at 0.05° grid resolution, almost half of the total global irrigable area
 375 occupies less than 25% of a grid cell.

376

377 The degree of concentration differs between countries for two reasons. Firstly, the true distribution of
 378 irrigation land varies; for example, irrigation tends to be highly concentrated in large surface water
 379 irrigation schemes (e.g., the Nile delta and Indus floodplains) but can be highly distributed where
 380 supplementary irrigation water is drawn from unregulated streams or groundwater. Secondly, the
 381 quality, resolution and predictive value of information related to irrigation area varies widely, which
 382 affects the accuracy of mapping (Portmann et al., 2010). The distribution of irrigation land introduces
 383 uncertainty in the attribution of E' in grid cells with small fractions of irrigated land. We expect that
 384 the fraction of a grid cell that needs to be irrigated to create a measurable LST signal may be around
 385 10% but will vary spatially depending on the LST contrast between irrigated and non-irrigated land.
 386 To account for this uncertainty, we calculated the mean I_0 (Eq. 4) per unit irrigation area for all grid
 387 cells with more than, respectively, 1, 2, 5, 10 and 25% of the area equipped for irrigation. These
 388 estimates were subsequently multiplied with the total area equipped for irrigation in each country. The
 389 coefficient of variation among the five estimates was calculated as a measure of estimation
 390 uncertainty.

391 The AQUASTAT database (FAO, 2017) provides country-level estimates of agricultural water
 392 withdrawal (W in $\text{km}^3 \text{y}^{-1}$) from surface and groundwater. **(Domestic and industrial withdrawals are**
 393 **not considered because a large fraction of these withdrawals is not evaporated but returned to the**
 394 **environment.)** The estimates are derived by different methods for different countries, and likely
 395 include both bottom-up and top-down techniques. Estimates also relate to different periods or years.
 396 Despite these uncertainties, they currently represent official international statistics for each country.

397 Any comparison of field-level irrigation water application (I_0) and large-scale water withdrawal (W)
398 needs to account for inefficiencies in the entire water distribution network. These include evaporation,
399 leakage and return flow on- and off-farm. ‘Project efficiencies’ that express the ratio of I_0 over W can
400 be estimated in principle, but this requires detailed ancillary data (Bos and Nugteren, 1990). In their
401 global modelling study, Siebert and Döll (2010) proposed ratios range from 0.25 for irrigation
402 dominated by paddy rice to 0.70 for efficient crop irrigation methods in Canada, Northern Africa and
403 Oceania. We did not assume values but instead calculated an ‘apparent’ bulk project efficiency for
404 each country, by dividing the ratio of modelled I_0 over W reported in AQUASTAT. The credibility of
405 the resulting values was subsequently interpreted within the framework developed by Bos and
406 Nugteren (1990).

407 *Secondary evaporation and the global water cycle*

408 Total secondary evaporation was estimated as the sum of open water evaporation plus the difference
409 $E' - E$, representing the difference between modelled primary evaporation E for a situation where
410 precipitation is the only source of water (the background estimate) and total evaporation E' resulting
411 from LST assimilation (the analysis estimate). The resulting estimate of total secondary evaporation is
412 a hypothetical and model-based quantity. Evaporation in the absence of lateral flows is counterfactual
413 and not necessarily accurately estimated by the model, particularly in humid environments.
414 Furthermore, all open water evaporation was included in secondary evaporation; we did not attempt to
415 estimate the evaporation that might have occurred from the surface had it not been covered by water.

416 The difference $E' - E$ was distributed dynamically in proportion to the magnitude of each of three
417 evaporation terms (i.e., transpiration, soil evaporation, and open water evaporation; wet canopy
418 evaporation was left unchanged). A component of secondary evaporation was attributed to irrigation
419 following the method described earlier. The remainder could be attributed to permanent water bodies,
420 ephemeral water bodies, and a residual component that includes any evaporation from replenished
421 wetlands and floodplains, as well as any use of groundwater sources beyond that simulated by the
422 model to occur from shallow groundwater (Peeters et al., 2013).

423

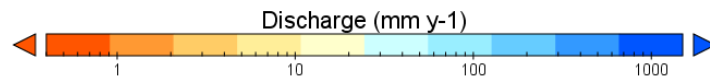
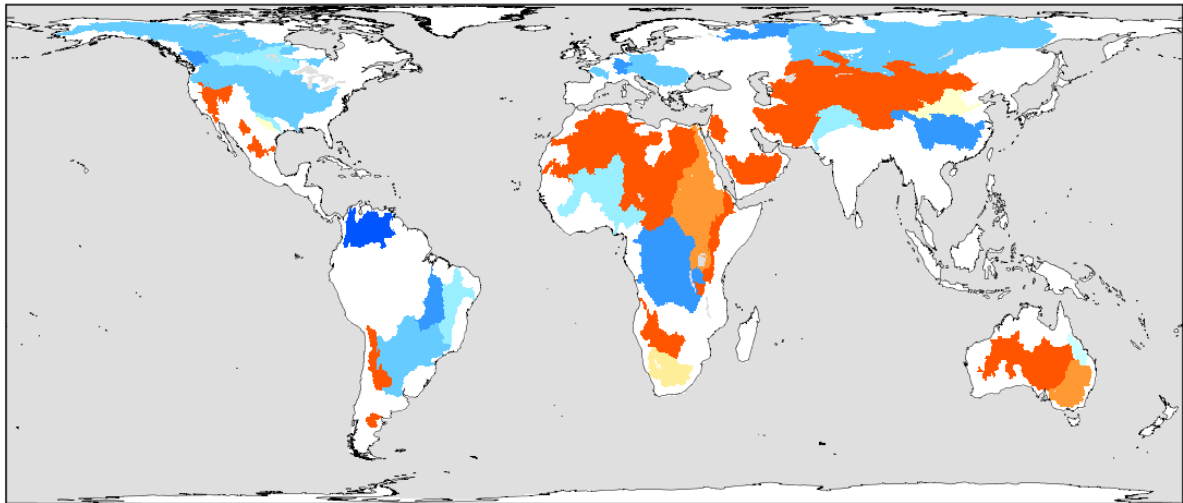
424 **Results**

425 *Basin water balance*

426 The combined surface area of the 51 basins used in evaluation (38 ocean-draining and 13 closed
427 basins) was 63 million km² or 47% of the ice-free land surface area (Figure 3Figure 4). For each
428 region, the period-average measured discharge (zero in the case of closed basins) was compared with
429 modelled Q_g and Q_n (Figure 4Figure 5, Table 1). Overall, accounting for secondary evaporation
430 produced a very small improvement in the correlation between observed and estimated discharge
431 (Figure 4Figure 5ab). However, the largest error contribution was from basins with high discharge

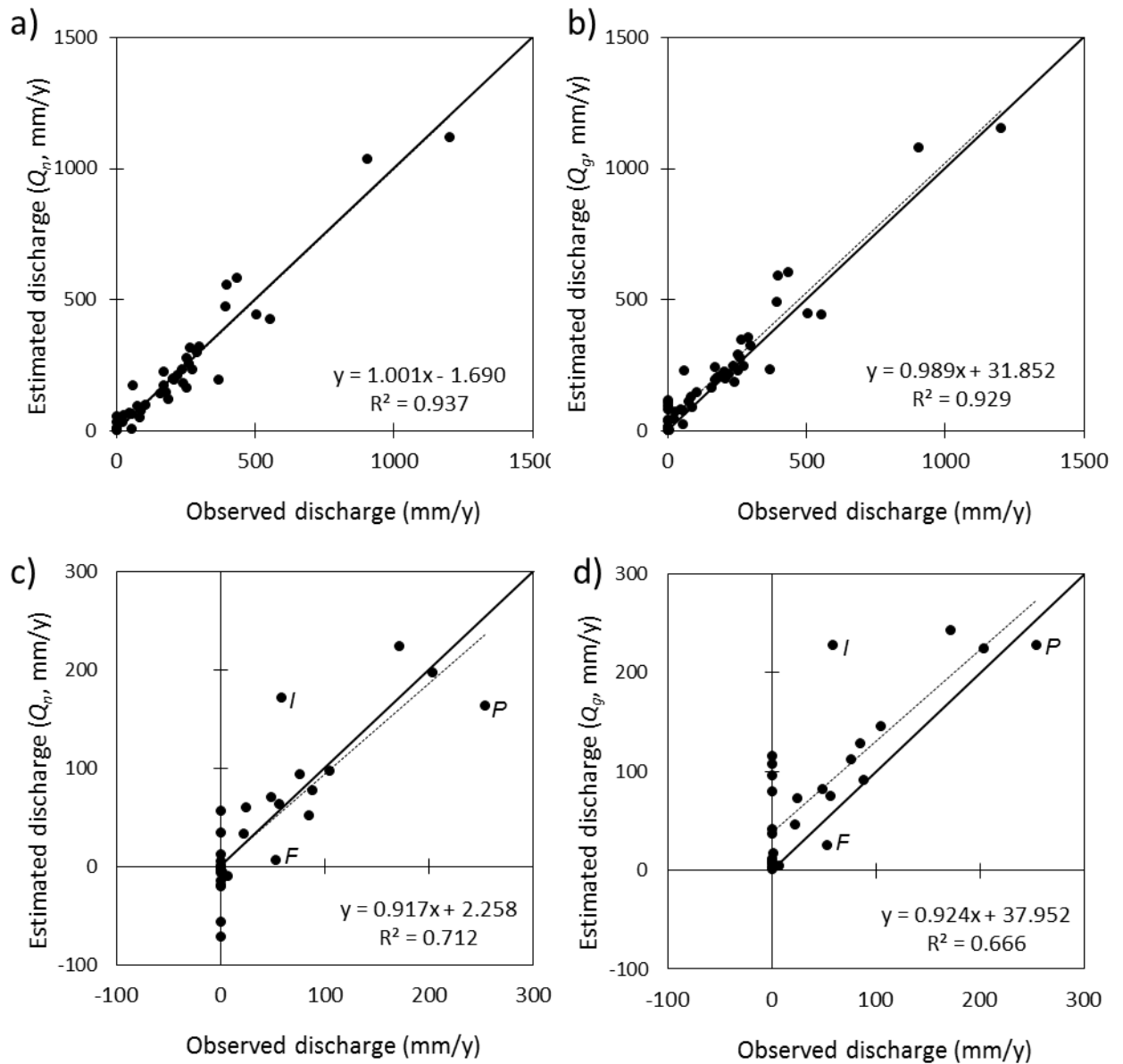
432 rates, where secondary evaporation represents a small fraction of Q_g . A clearer improvement in the
433 agreement was found for basins with less than 300 mm y^{-1} net discharge (Figure 4Figure 5cd). The
434 explained variance (R^2) increased from 0.67 to 0.71, and there was a reduction of the bias from +38 to
435 $+2 \text{ mm y}^{-1}$. Water balance estimates were improved considerably for several basins, including the
436 Indus River ('I' in Figure 4Figure 5cd), Nile River, the Great Basin in the USA, and the African Rift
437 Valley (Table 1). The agreement could not improve where Q_g estimates were already lower than
438 observed, such as the Paraná and Fitzroy Rivers ('P' and 'F' in Figure 4Figure 5cd). Water balance
439 estimates for some closed basins were also degraded, evident from negative Q_n values (e.g., the South
440 Interior and Rukwa basins in Southern Africa), implying that Q_g was underestimated, secondary
441 evaporation overestimated, or both (Table 1).

442



443

444 | **Figure 3** **Figure 4**. Extent and area-average annual discharge for the 38 ocean-draining (orange to blue) and 13
445 closed basins (dark orange) used in the evaluation. The two darkest blue colours indicate a discharge in excess
446 of 300 mm y⁻¹.



447

448 **Figure 5.** Comparison of observed basin-average discharge (mm y^{-1}) for large basins that are internally
 449 draining (i.e., zero discharge) or have adequate station discharge data with model estimates of (a) net discharge
 450 (Q_n), that is, gross discharge (Q_g) minus secondary evaporation, and (b) Q_g only. (c) and (d) data for discharge
 451 below 300 mm y^{-1} only (cf. Table 1). Letters indicate Indus (I), Paran (P), and Fitzroy (F) River.

452

453 Table 1. Area-average discharge (mm y^{-1}) for selected basins as observed and estimated by the model in the
 454 presence (Q_n) and absence (Q_g) of secondary evaporation, respectively. Listed data for basins with discharge
 455 less than 300 mm y^{-1} only (cf. [Figure 4](#)[Figure 5cd](#)).

Area-average basin discharge (mm y^{-1})	estimated		
	Observed	Q_n	Q_g
<i>Closed river basins</i>			
Great Basin, US	-	1	42
Guzman, North America	-	-6	3
Mairan-Viesca, Mexico	-	-15	7
Patagonia, South America	-	5	10
Titicaca-Chiquita, South America	-	-19	38
North Interior, Africa	-	-4	4
South Interior, Africa	-	-71	12
Rukwa, Africa	-	-56	115
Rift Valley, Africa	-	35	107
Jordan	-	-1	8
Arabian peninsula	-	0	1
Central Asia	-	57	80
Central Australia	-	-20	8
<i>Ocean-reaching rivers</i>			
Nile, Africa	0	13	96
Murray, Australia	1	-5	17
Orange/Senqu, Africa	7	-9	4
Colorado, US	23	33	46
Huanghe, China	24	61	73
Burdekin, Australia	48	70	82
Parnaiba, Brazil	76	94	113
Brazos, US	57	64	76
Fitzroy, Australia	54	6	26
Indus, Asia	58	172	228
Sao Francisco, Brazil	105	97	146
Niger/Issa Ber, Africa	88	78	92
Nelson, Canada	85	52	129
Paraná, South America	255	163	228
Elbe/Labe, Europe	172	224	243
Mississippi, US	204	198	225

456

457

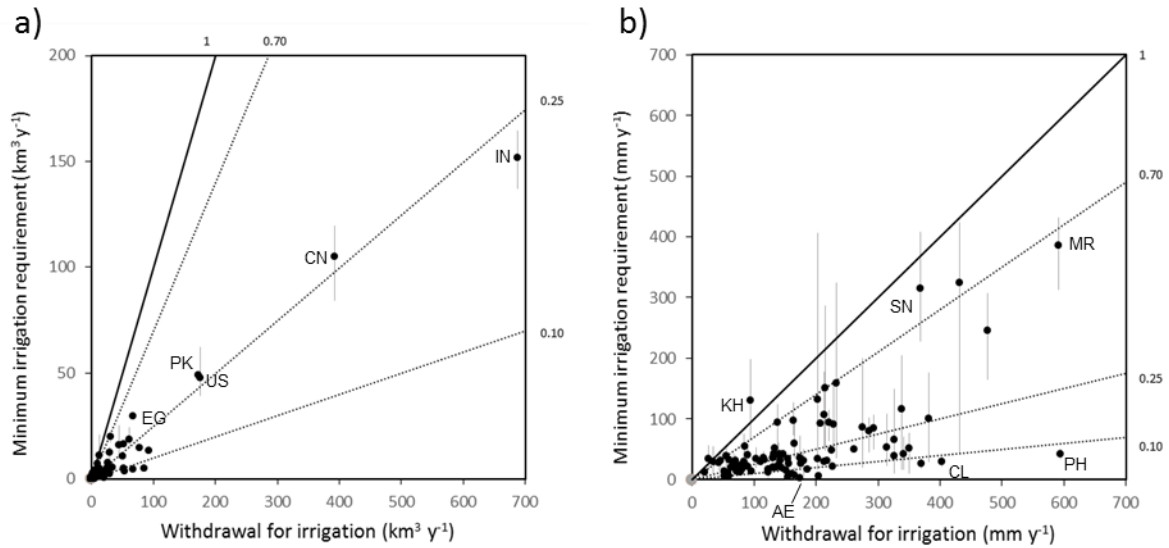
458 *Irrigation water requirements*

459 Spatiotemporal estimates of I_0 at 0.05° and daily time step were aggregated to country-level estimates
 460 in km³ y⁻¹ (Table 2). Also calculated were the coefficient of variation in I_0 estimates (CV_{I_0}) caused by
 461 the treatment of ‘mixed pixels’ in irrigation mapping, FAO-reported annual W , and the apparent
 462 project irrigation efficiency. Global I_0 for 2001–2014 was 680 km³ y⁻¹ (standard deviation 110 km³ y⁻¹)
 463 ¹). This value is lower than estimates of contemporary irrigation water use reported in the literature of
 464 1092 km³ y⁻¹ (Döll and Siebert, 2002), 1180 km³ y⁻¹ (Siebert and Döll, 2010) and 994–1179 km³ y⁻¹
 465 (Wada et al., 2014). Estimates of I_0 listed for seven countries by Döll and Siebert (2002) were all
 466 higher than those found here (Table 2), and even more than double for the USA (112 vs. 48 km³ y⁻¹)
 467 and Spain (21 vs 5.1 km³ y⁻¹). Quoted independent estimates were 113 km³ y⁻¹ for the USA (Solley et
 468 al., 1998) and 15 km³ y⁻¹ for Spain (J.A. Ortiz cited in Döll and Siebert, 2002).

469

470 Table 2. Irrigation water withdrawal (W) as reported to FAO for the 20 countries with largest agricultural
 471 withdrawals, along with the estimated minimum field-level irrigation requirement (I_0), the coefficient of
 472 variation in I_0 estimates (CV_{I_0}) and the apparent project efficiency (I_0 / W).

Country	W km ³ y ⁻¹	I_0 km ³ y ⁻¹	CV_{I_0} -	I_0 / W -
India	688	152	0.07	0.22
China	392	105	0.13	0.27
United States of America	175	48	0.20	0.27
Pakistan	172	49	0.01	0.28
Indonesia	93	14	0.10	0.15
Iran	86	5	0.22	0.06
Viet Nam	78	15	0.05	0.19
Philippines	67	5	0.16	0.07
Egypt	67	30	0.02	0.44
Mexico	62	19	0.22	0.31
Japan	54	4	0.23	0.07
Iraq	52	5	0.19	0.10
Thailand	52	16	0.09	0.32
Uzbekistan	50	11	0.02	0.21
Brazil	45	16	0.39	0.36
Turkey	34	6	0.36	0.16
Bangladesh	32	20	0.08	0.63
Burma	30	13	0.21	0.43
Chile	29	2	0.22	0.07
Argentina	28	5	0.47	0.17
Global	2,767	680	0.16	0.25



473

474 **Figure 5Figure 6.** Comparison of country-level agricultural water withdrawal (W) (FAO, 2017) and estimated
 475 minimum irrigation requirement (I_0) expressed as (a) total volume, and (b) depth per unit area of area equipped
 476 for irrigation for countries with $>1 \text{ km}^3 \text{ y}^{-1}$ withdrawals ($N=91$). Dotted lines show apparent project efficiencies
 477 between the two quantities. Countries indicated are (in a) Egypt (EG), Pakistan (PK), United States (US), China
 478 (CN) and India (IN), and (in b) Cambodia (KH), Senegal (SN), Mauritania (MR), United Arab Emirates (AE),
 479 Chile (CL), and the Philippines (PH).

480

481 The I_0 explains 96% in the variance in W by country (Figure 5Figure 6a), but total variance is
 482 dominated by only four countries, and the area equipped for irrigation explains already explains 86%
 483 of the variance. Volumes were divided by the total area equipped for irrigation to normalise for these
 484 effects. Normalised I_0 explained 38% of the variance in normalised W (Figure 5Figure 6b). A high
 485 correlation between the two is not necessarily to be expected, as country-average project efficiencies
 486 will vary (represented by the lines in Figure 5Figure 6b). For example, a low efficiency is inferred and
 487 would be expected in the Philippines, where irrigation is dominated by paddy rice agriculture,
 488 whereas higher efficiencies would be expected in large schemes in arid countries such as Egypt and
 489 Mauritania. Nonetheless, apparent efficiencies are generally lower than would be expected based on
 490 benchmark estimates provided by Bos and Nugteren (1990). For example, using global volumes of I_0
 491 and W , a project efficiency of 0.25 is calculated. This is lower than estimates of 0.36–0.43 assumed in
 492 previous studies (Döll and Siebert, 2002; Wada et al., 2014; Siebert and Döll, 2010). Physically
 493 impossible or implausible project efficiencies were also calculated for some countries, including
 494 Cambodia ($I_0/W > 1$), and the United Arab Emirates and Chile ($I_0/W < 0.1$) (Figure 5Figure 6b).
 495 Possible explanations for this will be discussed.

496

497 *Secondary evaporation and the global water cycle*

498 We estimate that secondary evaporation contributed 41.2 mm y⁻¹ or 8.1% to total evaporation from the
 499 global land area during 2001–2014 (Table 3), equivalent to 5.4% of terrestrial precipitation (759 mm
 500 y⁻¹) and 16% of generated streamflow (258 mm y⁻¹). Globally, only a very small percentage of all
 501 secondary evaporation (5%) was due to irrigation. Overall more important pathways for secondary
 502 evaporation were evaporation from permanent water bodies (48%), enhanced transpiration associated
 503 with wetland vegetation or greater-than-predicted groundwater uptake (27%), enhanced soil
 504 evaporation (11%), and evaporation from ephemeral water bodies (10%). Surface and groundwater
 505 inputs enhance global plant transpiration by an estimated 12.1 mm y⁻¹, representing a 4.4% increase.
 506 Of this increase, 10% can be attributed to irrigation.

507

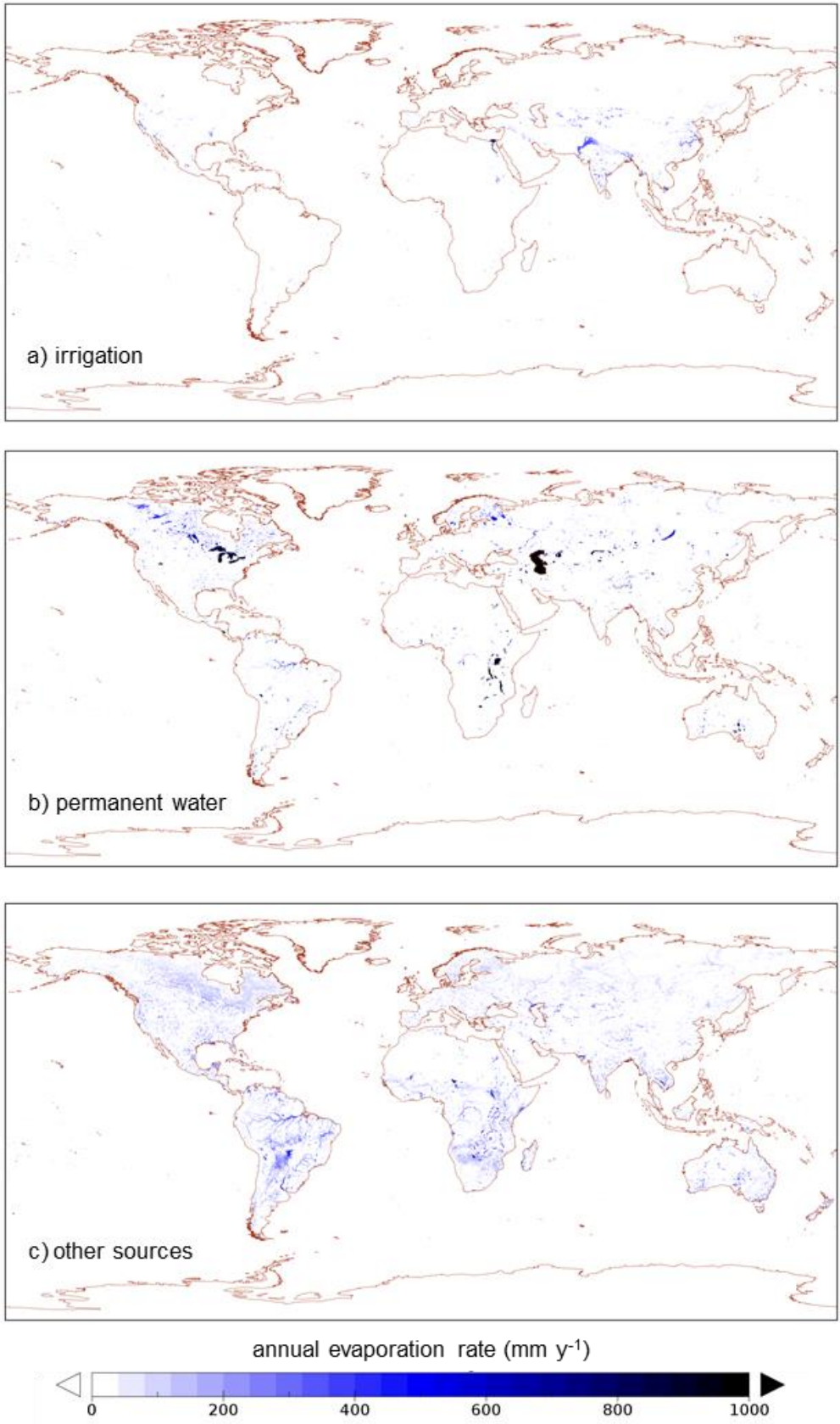
508 Table 3. Estimates of annual primary and secondary evaporation (*E* in mm y⁻¹) components for 2001-
 509 –2014 expressed as water depths across the global terrestrial area (149·10⁶ km²).

	Primary E	Secondary E	Total	Irrigation only
wet canopy E	81.3	–	81.3	–
transpiration	278.7	12.1	290.8	1.2
soil E	107.0	4.9	111.9	0.5
E from ephemeral water	–	4.6	4.6	0.3
E from permanent water	–	19.6	19.6	–
Total	467.0	41.2	508.2	2.0

510

511 The spatial distribution of evaporation from irrigation areas ([Figure 6](#)[Figure 7a](#)) and permanent water
 512 bodies ([Figure 6](#)[Figure 7b](#)) largely reflects the irrigation and water mapping input data, respectively.
 513 The spatial distribution of other sources of secondary evaporation provides some new insights ([Figure](#)
 514 [6](#)[Figure 7c](#)). Globally, some areas with the greatest secondary evaporation volumes include receiving
 515 floodplains in tropical monsoonal regions. The main regions in South America include the Gran
 516 Chaco and Pantanal plains and Amazon floodplains ([Figure 7](#)[Figure 8](#)). The main regions in Africa
 517 the Southern Interior basin in Botswana and surrounding countries (including the Okavango Delta and
 518 other wetlands), and the floodplains of the White Nile River in South Sudan and the Inner Niger Delta
 519 ([Figure 8](#)[Figure 9](#)). Other areas with high secondary evaporation rates include the Yucatan peninsula
 520 in Mexico ([Figure 7](#)[Figure 8](#)), the boreal wetlands and ephemeral lakes of Canada and Scandinavia
 521 ([Figure 7](#)[Figure 8](#) and [Figure 8](#)[Figure 9](#), respectively), and the salt lakes and floodplains of inland
 522 Australia ([Figure 9](#)[Figure 10](#)).

523

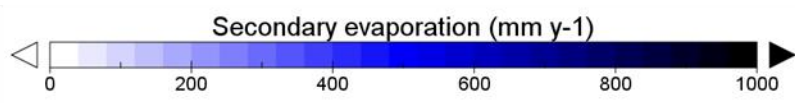
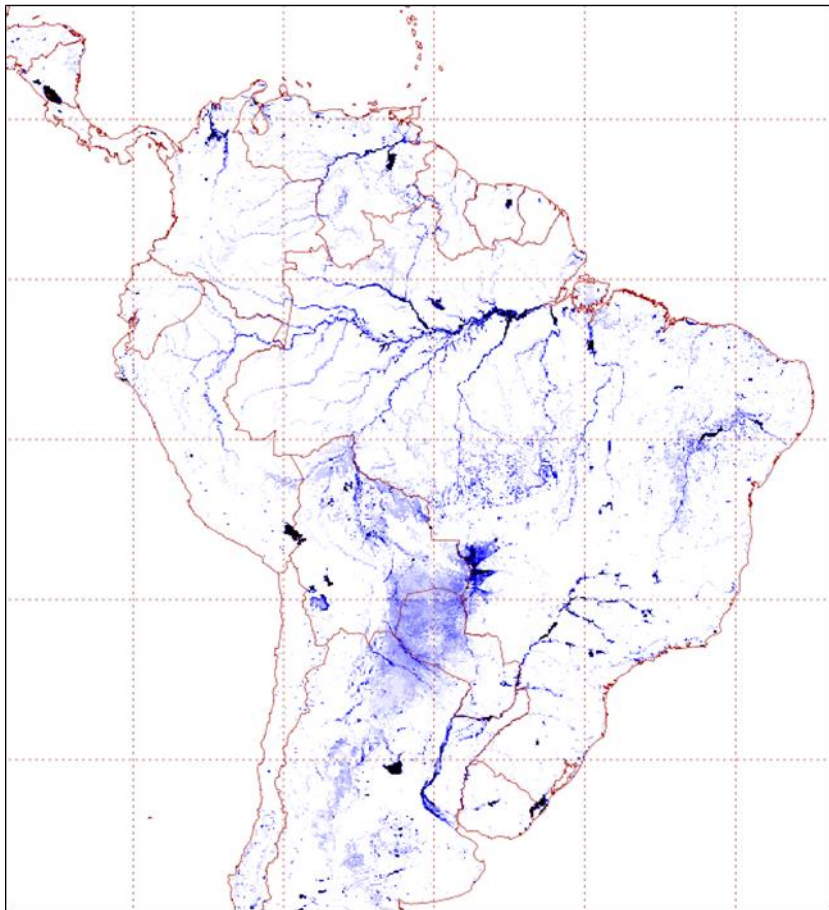
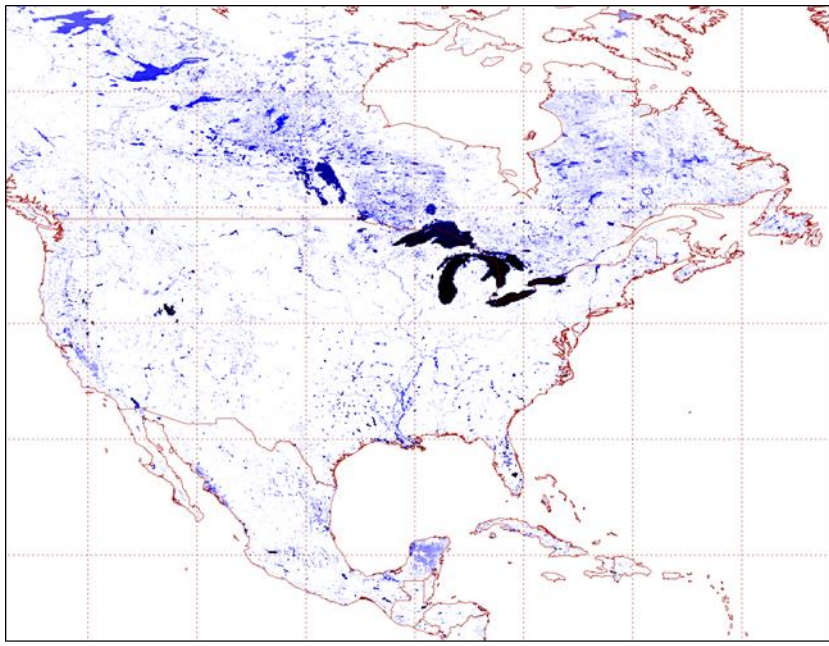


524

525

526

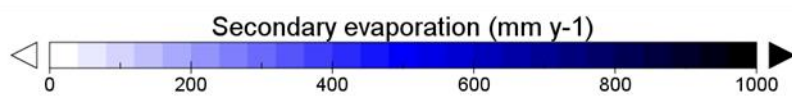
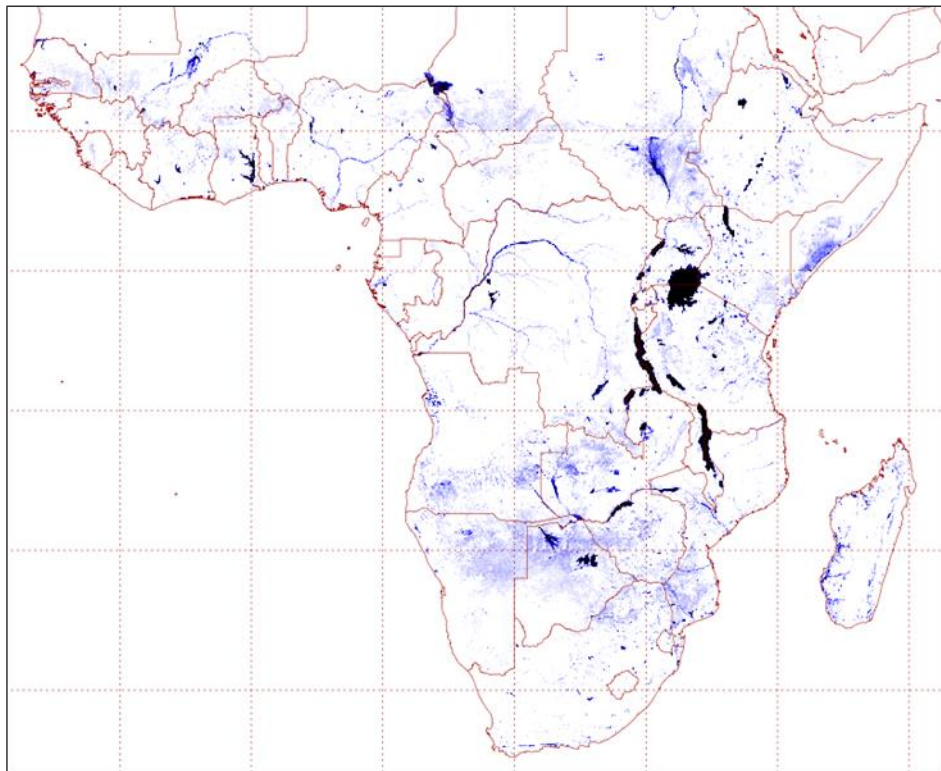
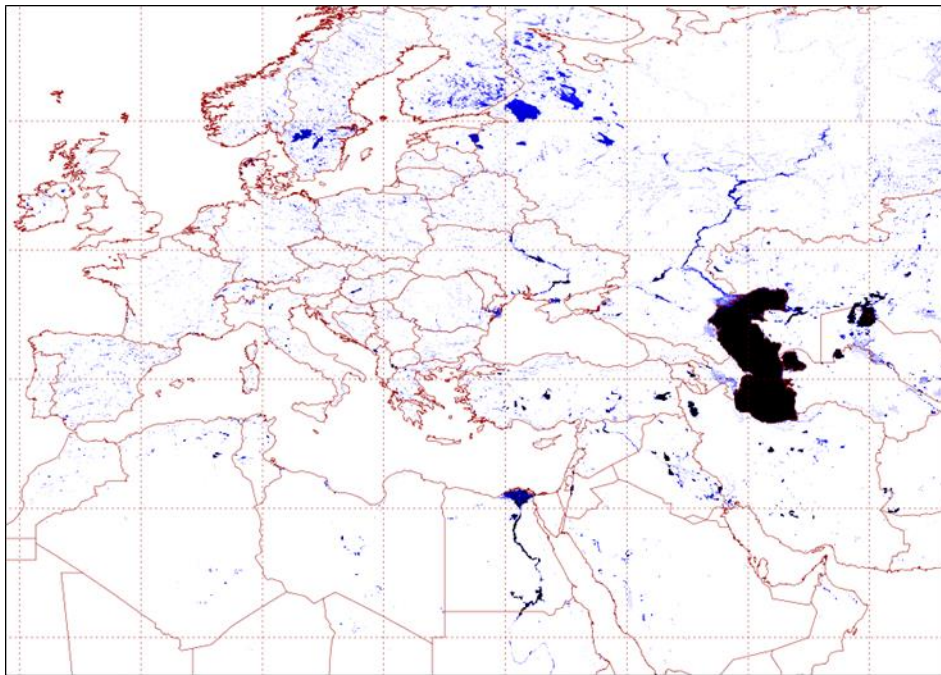
Figure 6 **Figure 7.** Spatial distribution of estimated secondary evaporation losses derived from (a) irrigation, (b) permanent water bodies, and (c) other sources, including wetlands and floodplains.



527

528 ~~Figure 7~~ **Figure 8.** Spatial distribution of secondary evaporation losses in the Americas.

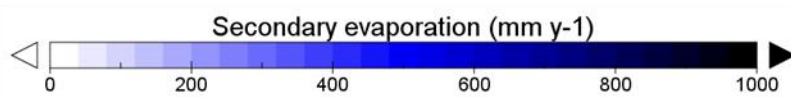
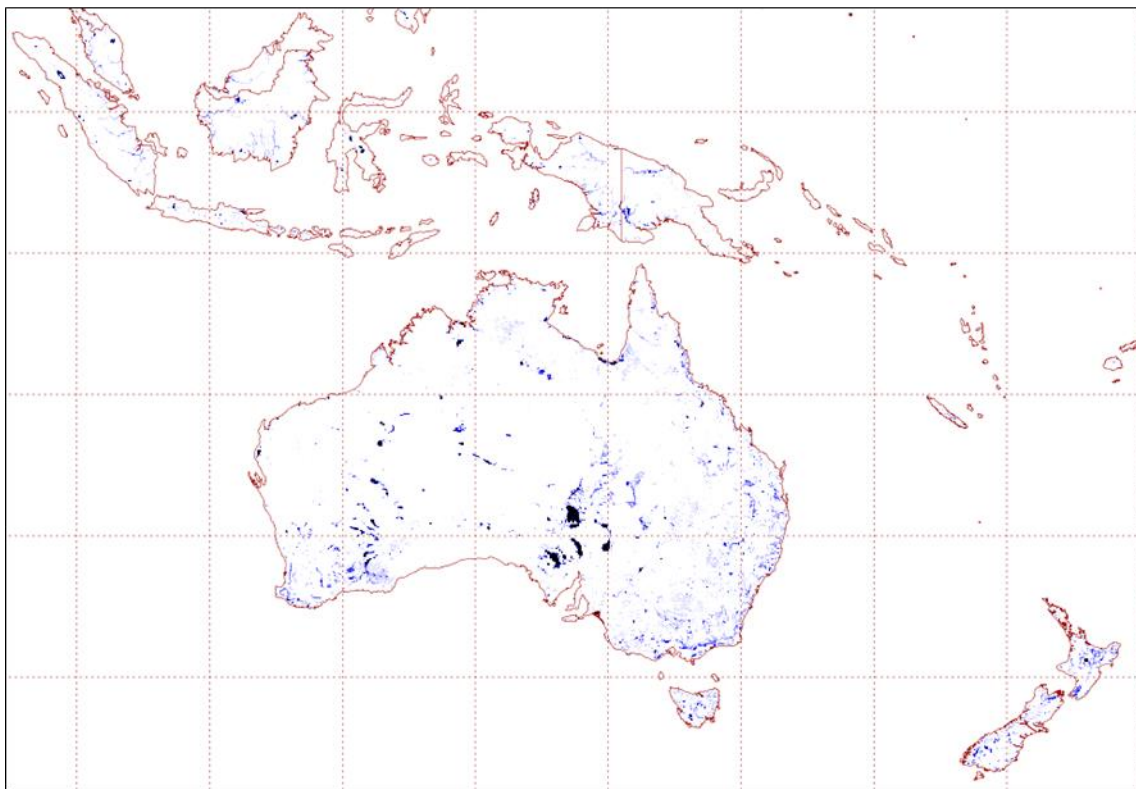
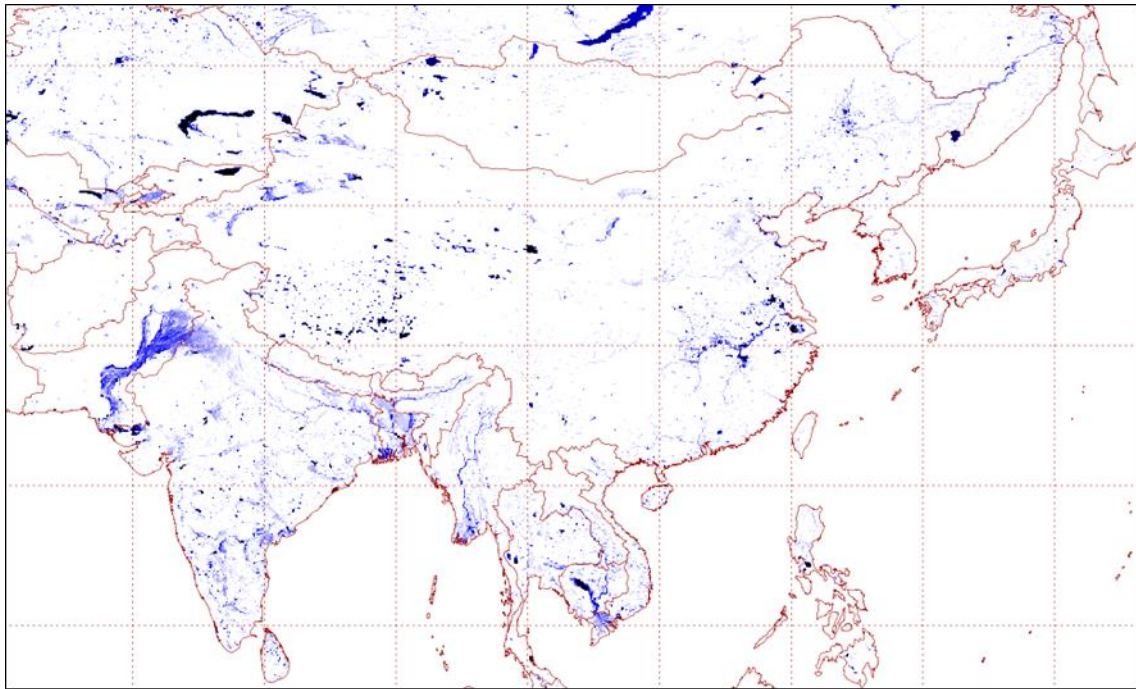
529



530

531 | [Figure 8](#)[Figure 9](#). Spatial distribution of secondary evaporation losses in Eurasia and Africa.

532



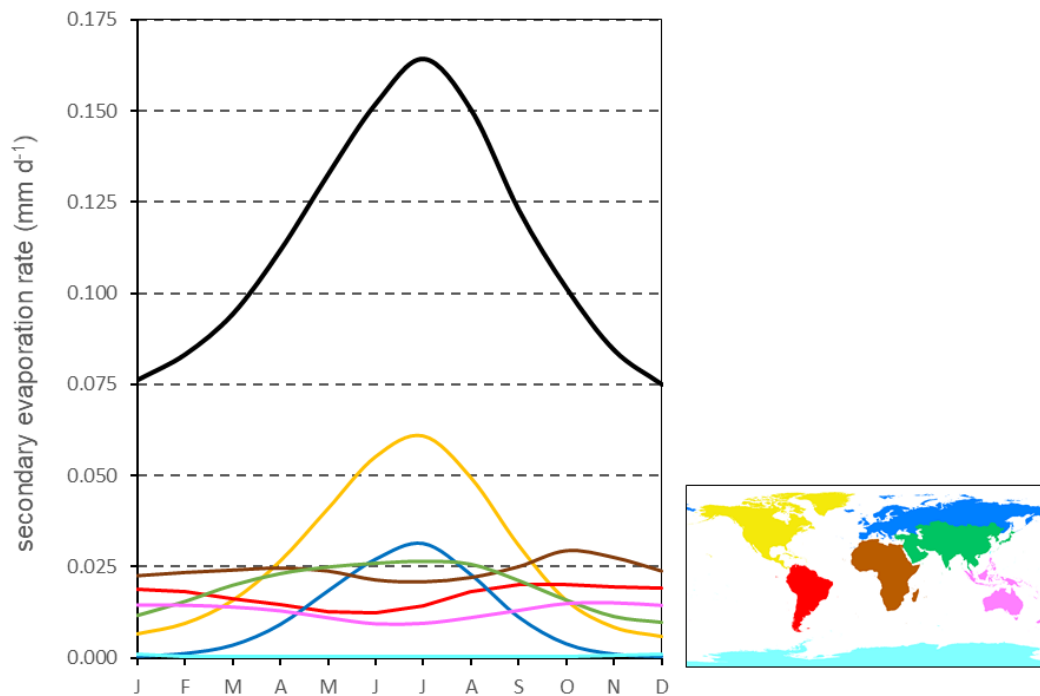
533

534 **Figure 9** **Figure 10.** Spatial distribution of secondary evaporation losses in Eastern Asia and Oceania.

535

536 There is a pronounced seasonal cycle in secondary evaporation at global scale (Figure 11). The rate of
 537 secondary evaporation is more than two times higher in northern summer than in northern winter.
 538 This is primarily due to the greater rate of evaporation from the many surface water bodies in
 539 formerly glaciated regions, including the American Great Lakes, as well as a higher rate of
 540 evaporation from the Caspian Sea. By contrast, secondary evaporation in regions located wholly or
 541 partially in the southern hemisphere show a much less pronounced seasonal cycle and a greater
 542 influence of water availability. Averaged over time, each of the regions considered makes a similarly
 543 sized contribution to secondary evaporation globally (10–24%) with the exception of Antarctica
 544 (0.4%).

545



546

547 Figure 11. Average (2001–2012) seasonal cycle of secondary evaporation at global scale (black line) and the
 548 contribution from different regions (colours corresponding to the map). All rates are expressed in mm d⁻¹ for the
 549 global land area.

550

551 **Discussion**

552 *Uncertainties in evaporation estimation*

553 The uncertainty in estimates of secondary evaporation arises from three main sources: (1) estimation
554 of ‘background’ evaporation E ; (2) estimation of surface water evaporation; and (3) estimation of total
555 evaporation E' by LST assimilation. A formal assessment of error in each of these terms is not
556 possible for lack of observations and will vary in space and time. Below we discuss what we expect to
557 be the main sources of uncertainty in each component.

558 An error in background model E may be compensated by data assimilation, but still leads to an error
559 in the estimated secondary evaporation, calculated as $E'-E$. The main sources of error in E vary as a
560 function of environmental conditions and the quality and density of the measurement network on
561 which the meteorological forcing data are based. In water-limited environments, the most likely
562 sources of error in E are errors in precipitation estimates and the simulation of water availability in the
563 root zone. The quality of precipitation estimates is relatively poor in many of the world’s dry regions
564 (Beck et al., 2017). Information on the ability of vegetation to access deeper soil moisture and
565 groundwater is important, particularly in ephemerally wet systems, but is not available at the global
566 scale. In humid environments, the most likely sources of error in E are in the estimation of rainfall
567 interception losses, the net available energy for evaporation, and surface conductance. As part of
568 earlier model development, background E was compared with estimates derived from flux tower
569 observations and compared with alternative ET estimation methods (Yebra et al., 2013; ~~Van Dijk,~~
570 ~~unpublished and supplement to this article~~). These evaluations showed little if any no systematic bias
571 in E and a standard difference of 135–168 mm y^{-1} across sites (~~$N=16-168$~~). This total difference also
572 includes errors in the flux tower-derived estimates (e.g., due to a lack of energy balance closure) and
573 differences arising because the tower footprint is not representative of the grid cell. ~~Therefore the true~~
574 ~~error in our estimates will be lower.~~

575 Observation-based estimates of large-area evaporation from water bodies, wetlands and irrigated areas
576 (i.e. $>0.05^\circ$) are scarce. Some site measurements of wetland and irrigation evaporation have been
577 published (e.g., Guerschman et al., 2009) but typically reflect an environment with very high spatial
578 variation and therefore often cannot easily be compared to estimates at 0.05° . A coordinated effort
579 that collates observations of secondary evaporation and combines these with historical time series
580 remote sensing imagery (cf. Figure 1a) to generate estimates at a more representative spatial scale
581 would appear necessary and valuable.

582 Errors in the estimation of surface water evaporation are the combined result of errors in the
583 estimation of open water evaporation rate and the mapping of surface water extent. Open water
584 evaporation rate was estimated using the Priestley and Taylor (1972) approach. An important
585 uncertainty in this approach is that it does not account for strong contrasts in near-surface water
586 temperature. Surface water extent was mapped using 8-day MODIS shortwave infrared (SWIR)
587 reflectance composites (Van Dijk et al., 2016). Systematic overestimation of water extent can occur in
588 low relief regions with very low SWIR reflectance (e.g., lava outflows fields), whereas
589 underestimation can occur in regions with a dense elevated canopy that prevents water detection (e.g.,

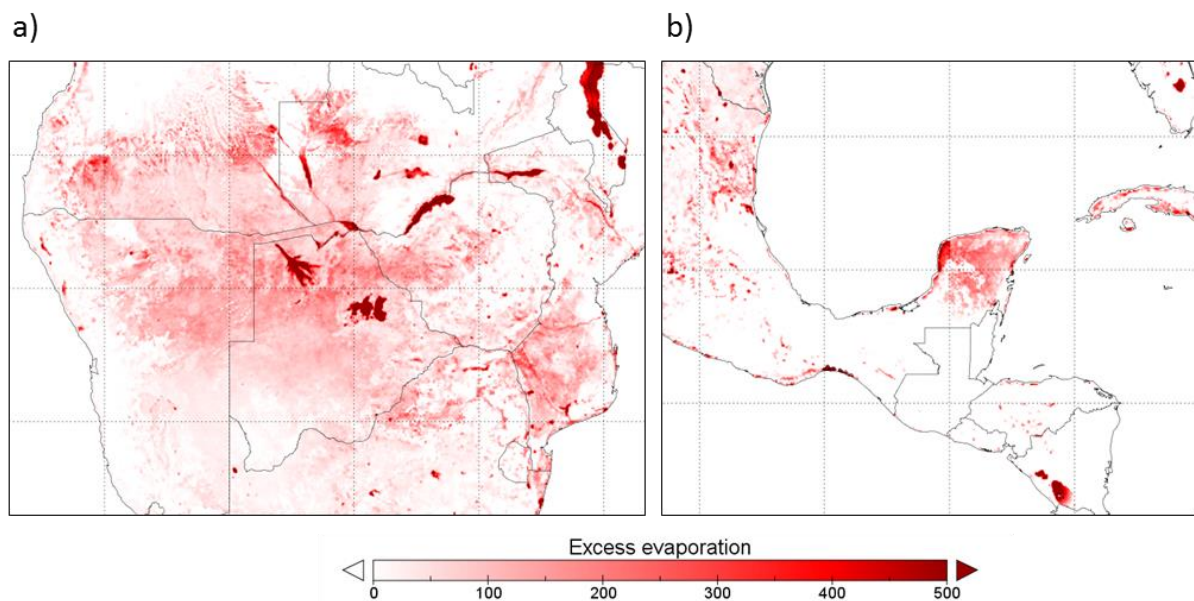
590 floodplain forests or mature flooded crops). Values of the updated $\lambda E'$ were constrained to positive
591 values below or equal to potential evaporation E_0 , and therefore any gross underestimation of E_0 by
592 the model due to errors in meteorological forcing data would have resulted in an underestimation of
593 the true evaporation rate.

594 The LST assimilation mitigates estimation errors in background and open water evaporation but is
595 also subject to uncertainties of its own. The technique developed here relies on the assumption that
596 there is a perfect correlation between spatial LST anomalies at the time-of-overpass (around 10 am
597 local time) and daytime (sunrise-sunset) average values, or at least for the low-relief areas where LST
598 was assimilated. A systematic bias in the global estimates of governing variables (radiation, air
599 temperature and humidity, wind speed) are likely to be less problematic than spatially variable
600 differences in those low-relief areas. In reality, ~~there can be~~ spatial differences in the temporal rate
601 of LST change can arise, for example, ~~as a function of from~~ spatial differences in heat storage
602 capacity and aerodynamic conductance (Kalma et al., 2008). Furthermore, we assumed a constant,
603 maximum bias-adjusted error of 1K in the difference between observed and model background LST.
604 Each of these choices ~~can~~ could have affected the efficacy of the assimilation.

605 Nonetheless, assessment of temporal patterns in E' (such as in Figure 1e) and the spatial patterns in
606 secondary evaporation (Figures 6–9) agree with known areas receiving lateral inflows (e.g., wetlands)
607 or irrigation. Less expected were the widespread high secondary evaporation rates in the northern
608 Yucatan peninsula in Mexico and the Southern Interior in Southern Africa. The northern Yucatan
609 peninsula is a low lying region with karst geology and forest are known to access shallow
610 groundwater (Bauer-Gottwein et al., 2011). The Southern Interior includes several terminal wetlands
611 (e.g., the Okavango Delta) and has unconsolidated alluvial deposits that contain productive aquifers
612 (MacDonald et al., 2012) and it is plausible that at least some of the vegetation has access to deeper
613 soil moisture or groundwater. In both cases, the background evaporation estimate (E) is constrained
614 by precipitation and the corresponding simulated presence of soil- and groundwater within the root
615 zone (E). Any underestimation of E leads to an increased estimate $E'-E$ and therefore an increased
616 estimate of secondary evaporation, without necessarily implying that all the water involved is derived
617 from later inflows. An alternative measure of the importance of secondary evaporation is $E'-P$ (Figure
618 ~~1011~~). These results suggest that period-average E' exceeds P by in the order of 100 to 200 mm y^{-1} .
619 For the Southern Interior basin, we found an apparent overestimation of c. 72 mm y^{-1} (Table 1) which
620 suggests that at least some of this difference is realistic. Underestimation of precipitation may also go
621 some way towards explaining these differences: ~~both regions are in transitional climates with a~~
622 ~~relatively strong, non-orographic precipitation gradient of 900–1400 mm y^{-1} (Yucatan) and 400–1100~~
623 ~~mm y^{-1} (Southern Interior), respectively. Combined with a low density of rainfall gauges (Hijmans et~~
624 ~~al., 2005), these gradients make a systematic bias in rainfall estimates more plausible. We analysed~~
625 ~~global water cycle reanalysis data that integrated GRACE gravity observations in an earlier study~~
626 ~~(Van Dijk et al., 2014) for a largely overlapping period (2003–2012) to test this. For the African~~

627 Southern Interior, the reanalysis demonstrated a clear increasing trend in subsurface storage (+12.3
 628 mm y⁻¹) that was not reproduced by an ensemble of models (+2.0 mm y⁻¹). This suggests that the
 629 global precipitation estimates used by models were indeed too low for this period, as also concluded
 630 by Van Dijk et al. (2014). For the Yucatan peninsula, a slight storage decrease (-3.3 mm y⁻¹) was
 631 inferred from the reanalysis, whereas the model ensemble suggested a slight increase (2.7 mm y⁻¹).
 632 This does not suggest any underestimation of precipitation. A net use of groundwater does appear
 633 plausible in this case, though likely not enough to explain the secondary evaporation rates estimated
 634 here.

635



636

637 Figure-Figure 1240. Mean difference between total evaporation and precipitation for 2001–2014 for (a)
 638 Botswana and (b) the Yucatan peninsula, and surrounding areas.

639

640 *Uncertainty in irrigation water requirement estimation*

641 The total estimate of minimum irrigation water requirement (I_0) at the global scale was about a third
 642 lower than previous model-based estimates (Siebert et al., 2010; Wada et al., 2014; Siebert and Döll,
 643 2010). There are some likely explanations for this. Firstly, the diffuse distribution of areas equipped
 644 for irrigation (Figure 2Figure 3) means that the LST signal from irrigation will likely have been too
 645 small to estimate the associated I_0 correctly everywhere. An insufficient LST signal is most likely for
 646 grid cells and countries with a temperate and humid climate and highly distributed irrigation, such as
 647 the US, where our estimate of I_0 was twice smaller than published previously. Conversely, irrigation
 648 evaporation estimates should be more accurate in hot, arid regions with large and concentrated
 649 irrigation, such as Egypt's Nile Delta (Figure 1). The temporal pattern of the evaporative fraction for
 650 this grid cell corresponds well with that of vegetation cover (Figure 1e) and assumes values that

651 appear realistic, even more so when considering that only around 80% of the grid cell was irrigated
652 (Figure 1a).

653 Second, previous studies have estimated crop water use (and from that, I_0) using the FAO method of
654 Allen et al. (1998). This method assumes a well-growing crop not affected by ineffective or
655 insufficient irrigation, unfavourable weather, nutrition or soil, pests and diseases, or other growth-
656 limiting factors. The resulting crop water use estimates are likely to represent idealised conditions and
657 may be higher than actual water use.

658 Third, errors in irrigation area mapping are also likely to have played a role. It is noteworthy that the
659 MIRCA2000 mapping used here (Portmann et al., 2010) indicated that 100% of the grid cell in Figure
660 1a was equipped for irrigation. This is not the case: most unirrigated areas are settlements. Previous
661 studies will have assumed the entire area was available for irrigation and this difference alone would
662 cause their I_0 estimates for this particular grid cell to be 25% higher. While these numbers relate to
663 just a single grid cell, it serves to demonstrate that incorrect mapping of irrigation areas can have
664 considerable impact on our I_0 estimates. As another example, any irrigation outside the grid cells
665 indicated to have at least some irrigable area in the MIRCA2000 mapping would be wholly attributed
666 to non-irrigation forms of secondary evaporation.

667 Despite these caveats, it is highly likely that true irrigation water application is greater than our
668 estimate I_0 , as it was defined as a hypothetical quantity that might occur under conditions of optimally
669 efficient irrigation. Previous studies have made similar assumptions. In reality, field-level irrigation
670 efficiency is reduced by additional drainage below the root zone and any surface runoff that may
671 occur. Further uncertainties are introduced through the necessary assumptions about rooting depth and
672 root zone storage capacity. The comparison with FAO-reported W estimates suggests project
673 efficiencies that are lower than those assumed in previous studies, but the overall correlation between
674 country I_0 and W volumes was high, and could not solely be attributed to differences in irrigated area
675 (Figure 5Figure 6). A comparison of country I_0 and W expressed as area-average rates indicates
676 contrasts in project efficiency that are expected in several cases. In other cases, values are outside a
677 plausible range. At least some of these poor estimates are likely related to the mentioned inaccuracies
678 in irrigation mapping (e.g., Chile and the United Arab Emirates in Figure 5Figure 6b).

679 Overall, the method developed here shows a promising approach to estimate irrigation water use.
680 Estimation at an even higher spatial resolution should help to detect the LST signal more accurately
681 where irrigation areas are dispersed and so produce better estimates of E' . This provides a powerful
682 argument in support of 'hyper-resolution' water balance observation and modelling (Wood et al.,
683 2011). All satellite-derived inputs are available at a resolution that is about an order of magnitude
684 finer (500–1000 m) than used here, and computationally data assimilation at this resolution is also
685 already feasible. The main impediment is the resolution and quality of irrigation area mapping, which
686 is required to attribute secondary evaporation to irrigation and other sources. The E' estimates

687 themselves may assist in mapping, along with information on temporal vegetation patterns, open
688 water mapping and relief, among others. This is an avenue we hope to pursue in future.

689 *Importance of secondary evaporation in the global water cycle*

690 Our analysis suggests that secondary evaporation makes a meaningful contribution to global
691 evaporation (8.1%) and reduces the amount of discharge to the oceans by c. 16%. At the global scale,
692 irrigation is responsible for only a small fraction of this reduction (c. 5%), with the remainder
693 occurring from water bodies and wetlands. These global averages hide significant regional variation.
694 For example, irrigation plays an important role in the evaporation of river flows in the Nile, Indus and
695 Murray-Darling basins, where most of the discharge is evaporated before reaching the ocean. About
696 half of total global secondary evaporation is from permanent freshwater bodies, including from some
697 very large water bodies such as the Caspian Sea, the Great Lakes, and the African Rift Valley Lakes.

698 There is a strong seasonal cycle in secondary evaporation at global scale, driven by evaporation from
699 extensive surface water bodies in formerly glaciated regions in the northern hemisphere. This
700 illustrates the profound impact that glaciation has had on regional landscape hydrology, and its
701 influence at global scale.

702 We estimated global terrestrial evaporation to be 508 mm y^{-1} per unit land area or $75.5 \cdot 10^{12} \text{ m}^3 \text{ y}^{-1}$
703 total for 2001–2014, made up of 467 mm y^{-1} or $69.6 \cdot 10^{12} \text{ m}^3 \text{ y}^{-1}$ primary evaporation and 41.2 mm y^{-1}
704 or $6.1 \cdot 10^{12} \text{ km}^3 \text{ y}^{-1}$ secondary evaporation. This is close to estimates derived from previous studies.
705 For example, Miralles et al. (2016) reported 13 estimates of terrestrial E, derived from a variable
706 combination of satellite observations and modelling, with an average value of $69.2 \cdot 10^{12} \text{ km}^3 \text{ y}^{-1}$ and
707 coefficient of variation (CV) of $\pm 10\%$. Schellekens et al. (2017) reported a mean of $74.5 \cdot 10^{12} \text{ km}^3 \text{ y}^{-1}$
708 (CV of $\pm 6\%$) for an ensemble of 10 state-of-the-art global hydrological models and land surface
709 models. Some of these differences are attributable to the differences in total area and period
710 considered, but the different datasets also includes secondary evaporation losses to different degrees.
711 Given these represent 8% of total evaporation, such inconsistencies help to explain differences
712 between estimates.

713 The partitioning between primary evaporation components is within the range of recently published
714 estimates, though noting that those ranges are broad (Table 4). Secondary evaporation is fully
715 responsible for open water evaporation and has no impact on wet canopy evaporation; both are a
716 logical consequence of the way these terms are conceptualised. It is estimated that global transpiration
717 and soil evaporation are both enhanced by about 4.5% due to secondary evaporation of surface and
718 groundwater resources. Irrigation is responsible for a tenth of this increase, with the remainder due to
719 natural processes. Because of the coupling between transpiration and carbon uptake, it can be
720 assumed that these enhancements will increase global carbon uptake by a similar proportion. Once
721 again these small contributions apply at global scale, but there are strong differences locally and
722 regionally.

723

724 Table 4. Estimated percentage of total (or, between brackets, primary) terrestrial evaporation (E)
725 contributed by different pathways, compared with estimates from two recent studies.

Percent of total E	this study	Zhang et al. (2016)	Miralles et al. (2016)
wet canopy E	16 (17)	10	10-24
transpiration	57 (60)	65	24-76
soil E	21 (23)	25	14-52
open water E	4 (0)	-	-

726

727 Thiery et al. (2017) simulated the global impact of irrigation using coupled land surface and
728 atmosphere models. They estimated an evaporation increase from irrigation of $418 \text{ km}^3 \text{ y}^{-1}$; of similar
729 magnitude to the $300 \text{ km}^3 \text{ y}^{-1}$ we found. Despite this small contribution to total global evaporation,
730 their modelling did predict small but meaningful reductions in high-temperature extremes over and
731 near large irrigation areas; irrigation rates tend to be highest during hot and dry conditions. To the best
732 of our knowledge, there have been no studies on the impact of wetlands and water bodies on regional
733 and global climate so far. Given that we estimate these other forms of secondary evaporation to be
734 twenty times greater than from irrigation, their impact on the atmosphere should be significant.

735

736 **Conclusions**

737 We presented a methodology to assimilate thermal satellite observations into a global hydrological
738 model W3 at a resolution of 0.05° to estimate secondary evaporation of surface and groundwater
739 resources. In addition, we used a simple irrigation water balance model to estimate minimum
740 irrigation requirement (I_0) globally. Our main conclusions are as follows.

741 (1) The method developed produces realistic temporal and spatial patterns in secondary evaporation.
742 Accounting for secondary evaporation measurably improved water balance estimates for large closed
743 and open basins, reducing bias in the overall water balance closure from $+38$ to $+2 \text{ mm y}^{-1}$.

744 (2) Our I_0 estimates were lower than country-level estimates of irrigation water use produced by other
745 model estimation methods, for three reasons. Firstly, at the 0.05° resolution, much of global irrigated
746 land occupies only a small part of individual grid cells and may not reduce LST sufficiently to be
747 accurately estimated. Second, our I_0 estimates reflect actual evaporation, which can be lower than
748 idealised crop water use estimates used in previous studies. Third, spatial errors in irrigation area
749 mapping directly affect the attribution of secondary evaporation to irrigation. Overall, actual irrigation
750 application will most likely be higher than estimated here but possibly lower than reported previously.

751 (3) The role of irrigation water use in secondary evaporation is minor at the global scale, accounting
752 for 5% of total secondary evaporation and 0.4% of total terrestrial evaporation. Nonetheless, water
753 withdrawals and irrigation evaporation are an important part of the water balance in some regions.

754 (4) Around 16% of globally generated water resources evaporate before reaching the oceans or from
755 closed basins, enhancing total terrestrial evaporation by 8.8%. Of this secondary evaporation, 5% is
756 evaporated from irrigation areas, 58% from water bodies, and 37% from other surfaces.

757 (5) Lateral inflows of surface and water resources were estimated to increase global plant
758 transpiration by c. 4.5%. The impact on global carbon uptake would be expected to be of similar
759 magnitude. Previous studies have predicted that irrigation evaporation affects regional and global
760 climate. Given evaporation from wetlands and permanent water bodies is an order of magnitude
761 larger, their impact on the climate system should be pronounced.

762 There is scope for further improvement in accounting for natural and anthropogenic secondary losses
763 by applying the model-data assimilation approach developed here at higher resolution. This is
764 conceptually straightforward and computationally achievable. Key developments required include
765 more accurate and detailed dynamic observational data on surface water dynamics and more accurate
766 mapping of areas equipped for irrigation.

767 **Data availability**

768 The 5-km water balance estimates presented here are available via [http://www.wenfo.org/wald/data-](http://www.wenfo.org/wald/data-software/)
769 [software/](http://www.wenfo.org/wald/data-software/).

770

771 **Acknowledgements**

772 The MODIS products were retrieved from the online Data Pool, courtesy of the NASA EOSDIS Land
773 Processes Distributed Active Archive Center (LP DAAC), USGS/Earth Resources Observation and
774 Science (EROS) Center, Sioux Falls, South Dakota, https://lpdaac.usgs.gov/data_access/data_pool.
775 Albert van Dijk was supported under Australian Research Council's Discovery Projects funding
776 scheme (project DP140103679).

777

778 **Author contribution**

779 AVD conceptualised the study. JS, HB, AW and GD developed global input data for the modelling.
780 MY developed the remote sensing evaporation scheme. LR assisted in the development of the data
781 assimilation approach. AVD carried out the analysis and wrote the first draft manuscript. All other
782 authors contributed to the analysis, interpretation and writing.

783

784 **References**

- 785 Alcamo, J., Döll, P., Henrichs, T., Kaspar, F., Lehner, B., Rösch, T., and Siebert, S.: Development and testing of
786 the WaterGAP 2 global model of water use and availability, *Hydrological Sciences Journal*, 48, 317-337,
787 10.1623/hysj.48.3.317.45290, 2003.
- 788 Allen, R. G., Pereira, L. S., Raes, D., and Smith, M.: *Crop evapotranspiration - Guidelines for computing crop*
789 *water requirements.*, Food and Agricultural Organisation of the United Nations, Rome, 1998.
- 790 Anderson, M., Hain, C., Gao, F., Kustas, W., Yang, Y., Sun, L., Yang, Y., Holmes, T., and Dulaney, W.:
791 *Mapping evapotranspiration at multiple scales using multi-sensor data fusion*, 2016 IEEE International
792 *Geoscience and Remote Sensing Symposium (IGARSS)*, 2016, 226-229,
- 793 Bauer-Gottwein, P., Gondwe, B. R. N., Charvet, G., Marín, L. E., Rebolledo-Vieyra, M., and Merediz-Alonso,
794 G.: *Review: The Yucatán Peninsula karst aquifer, Mexico*, *Hydrogeology Journal*, 19, 507-524,
795 10.1007/s10040-010-0699-5, 2011.
- 796 Beck, H. E., de Roo, A., and van Dijk, A. I. J. M.: *Global Maps of Streamflow Characteristics Based on*
797 *Observations from Several Thousand Catchments*, *Journal of Hydrometeorology*, 16, 1478-1501, 10.1175/JHM-
798 D-14-0155.1, 2015.
- 799 Beck, H. E., van Dijk, A. I., de Roo, A., Miralles, D. G., McVicar, T. R., Schellekens, J., and Bruijnzeel, L. A.:
800 *Global- scale regionalization of hydrologic model parameters*, *Water Resources Research*, 2016.
- 801 Beck, H. E., van Dijk, A. I. J. M., Levizzani, V., Schellekens, J., Miralles, D. G., Martens, B., and de Roo, A.:
802 *MSWEP: 3-hourly 0.25° global gridded precipitation (1979–2015) by merging gauge, satellite, and reanalysis*
803 *data*, *Hydrol. Earth Syst. Sci.*, 21, 589-615, 10.5194/hess-21-589-2017, 2017.
- 804 Bicheron, P., Defourny, P., Brockmann, C., Schouten, L., Vancutsem, C., Huc, M., Bontemps, S., Leroy, M.,
805 Achard, F., and Herold, M.: *Globcover: products description and validation report*, in, ME, 2008.
- 806 Bos, M. G., and Nugteren, J.: *On irrigation efficiencies*, 19, ILRI, 1990.
- 807 Brooks, R., and Corey, A.: *Hydraulic Properties of Porous Media*, of Colorado State University Hydrology
808 *Paper*, 3, Colorado State University, 1964.
- 809 Dai, A., Qian, T., Trenberth, K. E., and Milliman, J. D.: *Changes in continental freshwater discharge from 1948*
810 *to 2004*, *Journal of Climate*, 22, 2773-2792, 2009.
- 811 Döll, P., and Siebert, S.: *Global modeling of irrigation water requirements*, *Water Resources Research*, 38,
812 2002.
- 813 Doody, T. M., Barron, O. V., Dowsley, K., Emelyanova, I., Fawcett, J., Overton, I. C., Pritchard, J. L., Van
814 Dijk, A. I. J. M., and Warren, G.: *Continental mapping of groundwater dependent ecosystems: A*
815 *methodological framework to integrate diverse data and expert opinion*, *Journal of Hydrology: Regional Studies*,
816 10, 61-81, <http://dx.doi.org/10.1016/j.ejrh.2017.01.003>, 2017.
- 817 Falkenmark, M., and Rockström, J.: *Balancing water for humans and nature: the new approach in ecohydrology*,
818 *Earthscan*, 2004.
- 819 *FAO: AQUASTAT database - Food and Agriculture Organization of the United Nations (FAO)*. Website
820 *accessed on 30/09/2017*, in, 2017.
- 821 Frost, A. J., Ramchurn, A., and Hafeez, M.: *Evaluation of the Bureau's Operational AWRA-L Model*,
822 *Melbourne*, 80, 2016a.
- 823 Frost, A. J., Ramchurn, A., and Smith, A. B.: *The Bureau's Operational AWRA Landscape (AWRA-L) Model*,
824 *Melbourne*, 47, 2016b.
- 825 Gleeson, T., Moosdorf, N., Hartmann, J., and Van Beek, L. P. H.: *A glimpse beneath earth's surface: GLobal*
826 *HYdrogeology MaPS (GLHYMPS) of permeability and porosity*, *Geophysical Research Letters*, 41, 3891-3898,
827 2014.

828 Glenn, E. P., Doody, T. M., Guerschman, J. P., Huete, A. R., King, E. A., McVicar, T. R., Van Dijk, A. I. J. M.,
829 Van Niel, T. G., Yebra, M., and Zhang, Y.: Actual evapotranspiration estimation by ground and remote sensing
830 methods: the Australian experience, *Hydrological Processes*, 25, 4103-4116, 10.1002/hyp.8391, 2011.

831 Guerschman, J. P., Van Dijk, A., Mattersdorf, G., Beringer, J., Hutley, L. B., Leuning, R., Pipunic, R. C., and
832 Sherman, B. S.: Scaling of potential evapotranspiration with MODIS data reproduces flux observations and
833 catchment water balance observations across Australia, *Journal of Hydrology*, 369, 107-119,
834 10.1016/j.jhydrol.2009.02.013, 2009.

835 Hijmans, R. J., Cameron, S. E., Parra, J. L., Jones, P. G., and Jarvis, A.: Very high resolution interpolated
836 climate surfaces for global land areas, *International Journal of Climatology*, 25, 1965-1978, 10.1002/joc.1276,
837 2005.

838 Holgate, C. M., De Jeu, R. A. M., van Dijk, A. I. J. M., Liu, Y. Y., Renzullo, L. J., Vinodkumar, Dharssi, I.,
839 Parinussa, R. M., Van Der Schalie, R., Gevaert, A., Walker, J., McJannet, D., Cleverly, J., Haverd, V.,
840 Trudinger, C. M., and Briggs, P. R.: Comparison of remotely sensed and modelled soil moisture data sets
841 across Australia, *Remote Sensing of Environment*, 186, 479-500, <http://dx.doi.org/10.1016/j.rse.2016.09.015>,
842 2016.

843 Hulley, G. C., Hughes, C. G., and Hook, S. J.: Quantifying uncertainties in land surface temperature and
844 emissivity retrievals from ASTER and MODIS thermal infrared data, *Journal of Geophysical Research:*
845 *Atmospheres*, 117, n/a-n/a, 10.1029/2012JD018506, 2012.

846 Kalma, J. D., McVicar, T. R., and McCabe, M. F.: Estimating land surface evaporation: a review of methods
847 using remotely sensed surface temperature data, *Surveys in Geophysics*, 29, 421-469, 10.1007/s10712-008-
848 9037-z, 2008.

849 Lehner, B., Verdin, K., and Jarvis, A.: New global hydrography derived from spaceborne elevation data, *Eos*,
850 *Transactions American Geophysical Union*, 89, 93-94, 2008.

851 MacDonald, A. M., Bonsor, H. C., Dochartaigh, B. É. Ó., and Taylor, R. G.: Quantitative maps of groundwater
852 resources in Africa, *Environmental Research Letters*, 7, 024009, 2012.

853 Melton, J. R., Wania, R., Hodson, E. L., Poulter, B., Ringeval, B., Spahni, R., Bohn, T., Avis, C. A., Beerling,
854 D. J., Chen, G., Eliseev, A. V., Denisov, S. N., Hopcroft, P. O., Lettenmaier, D. P., Riley, W. J., Singarayer, J.
855 S., Subin, Z. M., Tian, H., Zürcher, S., Brovkin, V., van Bodegom, P. M., Kleinen, T., Yu, Z. C., and Kaplan, J.
856 O.: Present state of global wetland extent and wetland methane modelling: conclusions from a model inter-
857 comparison project (WETCHIMP), *Biogeosciences*, 10, 753-788, 10.5194/bg-10-753-2013, 2013.

858 Miralles, D. G., Jiménez, C., Jung, M., Michel, D., Ershadi, A., McCabe, M. F., Hirschi, M., Martens, B.,
859 Dolman, A. J., Fisher, J. B., Mu, Q., Seneviratne, S. I., Wood, E. F., and Fernández-Prieto, D.: The WACMOS-
860 ET project – Part 2: Evaluation of global terrestrial evaporation data sets, *Hydrol. Earth Syst. Sci.*, 20, 823-842,
861 10.5194/hess-20-823-2016, 2016.

862 Nobre, A. D., Cuartas, L. A., Momo, M. R., Severo, D. L., Pinheiro, A., and Nobre, C. A.: HAND contour: a
863 new proxy predictor of inundation extent, *Hydrological Processes*, 2015.

864 Oki, T., and Kanae, S.: Global Hydrological Cycles and World Water Resources, *Science*, 313, 1068-1072,
865 10.1126/science.1128845, 2006.

866 Peeters, L. J. M., Crosbie, R. S., Doble, R. C., and Van Dijk, A. I. J. M.: Conceptual evaluation of continental
867 land-surface model behaviour, *Environmental Modelling & Software*, 43, 49-59,
868 <http://dx.doi.org/10.1016/j.envsoft.2013.01.007>, 2013.

869 Portmann, F. T., Siebert, S., and Döll, P.: MIRCA2000—Global monthly irrigated and rainfed crop areas around
870 the year 2000: A new high- resolution data set for agricultural and hydrological modeling, *Global*
871 *Biogeochemical Cycles*, 24, 2010.

872 Priestley, C. H. B., and Taylor, R. J.: On the assessment of surface heat flux and evaporation using large-scale
873 parameters, *Monthly Weather Review*, 100, 81-92, 1972.

874 Schellekens, J., Dutra, E., Martínez-de la Torre, A., Balsamo, G., van Dijk, A., Sperna Weiland, F., Minvielle,
875 M., Calvet, J. C., Decharme, B., Eisner, S., Fink, G., Flörke, M., Peßenteiner, S., van Beek, R., Polcher, J.,
876 Beck, H., Orth, R., Calton, B., Burke, S., Dorigo, W., and Weedon, G. P.: A global water resources ensemble of
877 hydrological models: the earth2Observe Tier-1 dataset, *Earth Syst. Sci. Data*, 9, 389-413, 10.5194/essd-9-389-
878 2017, 2017.

879 Shangguan, W., Dai, Y., Duan, Q., Liu, B., and Yuan, H.: A global soil data set for earth system modeling,
880 *Journal of Advances in Modeling Earth Systems*, 6, 249-263, 10.1002/2013MS000293, 2014.

881 Siebert, S., Burke, J., Faures, J. M., Frenken, K., Hoogeveen, J., Döll, P., and Portmann, F. T.: Groundwater use
882 for irrigation – a global inventory, *Hydrol. Earth Syst. Sci.*, 14, 1863-1880, 10.5194/hess-14-1863-2010, 2010.

883 Siebert, S., and Döll, P.: Quantifying blue and green virtual water contents in global crop production as well as
884 potential production losses without irrigation, *Journal of Hydrology*, 384, 198-217, 2010.

885 Simard, M., Pinto, N., Fisher, J. B., and Baccini, A.: Mapping forest canopy height globally with spaceborne
886 lidar, *Journal of Geophysical Research: Biogeosciences*, 116, 2011.

887 Solley, W. B., Pierce, R. R., and Perlman, H. A.: Estimated use of water in the United States in 1995, US
888 Geological Survey, 1998.

889 Thiery, W., Davin, E. L., Lawrence, D. M., Hirsch, A. L., Hauser, M., and Seneviratne, S. I.: Present-day
890 irrigation mitigates heat extremes, *Journal of Geophysical Research: Atmospheres*, 122, 1403-1422,
891 10.1002/2016JD025740, 2017.

892 Thom, A. S.: Momentum, Mass and Heat Exchange of Plant Communities, in: *Vegetation and the Atmosphere*,
893 edited by: Monteith, J. L., Academic Press, London, 57-109, 1975.

894 Tian, S., Tregoning, P., Renzullo, L. J., van Dijk, A. I. J. M., Walker, J. P., Pauwels, V. R. N., and Allgeyer, S.:
895 Improved water balance component estimates through joint assimilation of GRACE water storage and SMOS
896 soil moisture retrievals, *Water Resources Research*, 53, 1820-1840, 10.1002/2016WR019641, 2017.

897 [Van Dijk, A. I. J. M., and Bruijnzeel, L. A.: Modelling rainfall interception by vegetation of variable density](#)
898 [using an adapted analytical model. Part 1. Model description, *Journal of Hydrology*, 247, 230-238,](#)
899 [10.1016/S0022-1694\(01\)00392-4, 2001.](#)

900 Van Dijk, A. I. J. M.: AWRA Technical Report 3. Landscape Model (version 0.5) Technical Description,
901 WIRADA / CSIRO Water for a Healthy Country Flagship, Canberra, 2010.

902 [Van Dijk, A. I. J. M., Gash, J. H., van Gorsel, E., Blanken, P. D., Cescatti, A., Emmel, C., Gielen, B., Harman,](#)
903 [I. N., Kiely, G., Merbold, L., Montagnani, L., Moors, E., Sottocornola, M., Varlagin, A., Williams, C. A., and](#)
904 [Wohlfahrt, G.: Rainfall interception and the coupled surface water and energy balance, *Agricultural and Forest*](#)
905 [Meteorology, 214–215, 402–415, <http://dx.doi.org/10.1016/j.agrformet.2015.09.006>, 2015.](#)

906 Van Dijk, A. I. J. M., Brakenridge, G. R., Kettner, A. J., Beck, H. E., De Groeve, T., and Schellekens, J.: River
907 gauging at global scale using optical and passive microwave remote sensing, *Water Resources Research*, 52,
908 6404-6418, 10.1002/2015WR018545, 2016.

909 Van Niel, T. G., McVicar, T. R., Roderick, M. L., van Dijk, A. I. J. M., Renzullo, L. J., and van Gorsel, E.:
910 Correcting for systematic error in satellite-derived latent heat flux due to assumptions in temporal scaling:
911 Assessment from flux tower observations, *Journal of Hydrology*, 409, 140-148, 10.1016/j.jhydrol.2011.08.011,
912 2011.

913 Wada, Y., Wisser, D., and Bierkens, M. F. P.: Global modeling of withdrawal, allocation and consumptive use
914 of surface water and groundwater resources, *Earth System Dynamics*, 5, 15-40, 2014.

915 [Wallace, J., Macfarlane, C., McJannet, D., Ellis, T., Grigg, A., and van Dijk, A.: Evaluation of forest](#)
916 [interception estimation in the continental scale Australian Water Resources Assessment–Landscape \(AWRA-L\)](#)
917 [model, Journal of Hydrology, 499, 210-223, 2013.](#)

918 Wan, Z., Zhang, Y., Zhang, Q., and Li, Z. L.: Quality assessment and validation of the MODIS global land
919 surface temperature, International Journal of Remote Sensing, 25, 261-274, 10.1080/0143116031000116417,
920 2004.

921 Wan, Z.: New refinements and validation of the MODIS Land-Surface Temperature/Emissivity products,
922 Remote Sensing of Environment, 112, 59-74, 2008.

923 Wan, Z., and Li, Z. L.: Radiance- based validation of the V5 MODIS land- surface temperature product,
924 International Journal of Remote Sensing, 29, 5373-5395, 10.1080/01431160802036565, 2008.

925 Wan, Z.: MOD11C1 MODIS/Terra Land Surface Temperature/Emissivity Daily L3 Global 0.05Deg CMG
926 V006. , in, edited by: (<https://doi.org/10.5067/modis/mod11c1.006>), N. E. L. P. D., 2015.

927 Wang-Erlandsson, L., Bastiaanssen, W. G., Senay, G. B., van Dijk, A. I., Guerschman, J. P., Keys, P. W.,
928 Gordon, L. J., and Savenije, H. H.: Global root zone storage capacity from satellite-based evaporation,
929 Hydrology and Earth System Sciences, 20, 1459, 2016.

930 Weedon, G. P., Balsamo, G., Bellouin, N., Gomes, S., Best, M. J., and Viterbo, P.: The WFDEI meteorological
931 forcing data set: WATCH Forcing Data methodology applied to ERA- Interim reanalysis data, Water Resources
932 Research, 50, 7505-7514, 2014.

933 Wood, E. F., Roundy, J. K., Troy, T. J., van Beek, L. P. H., Bierkens, M. F. P., Blyth, E., de Roo, A., Döll, P.,
934 Ek, M., Famiglietti, J., Gochis, D., van de Giesen, N., Houser, P., Jaffé, P. R., Kollet, S., Lehner, B.,
935 Lettenmaier, D. P., Peters-Lidard, C., Sivapalan, M., Sheffield, J., Wade, A., and Whitehead, P.:
936 Hyperresolution global land surface modeling: Meeting a grand challenge for monitoring Earth's terrestrial
937 water, Water Resources Research, 47, W05301, 10.1029/2010WR010090, 2011.

938 Xiao, Z., Liang, S., Wang, J., Chen, P., Yin, X., Zhang, L., and Song, J.: Use of general regression neural
939 networks for generating the GLASS leaf area index product from time-series MODIS surface reflectance, IEEE
940 Transactions on Geoscience and Remote Sensing, 52, 209-223, 2014.

941 Yebra, M., Van Dijk, A., Leuning, R., Huete, A., and Guerschman, J. P.: Evaluation of optical remote sensing to
942 estimate actual evapotranspiration and canopy conductance, Remote Sensing of Environment, 129, 250-261,
943 2013.

944 Yebra, M., Van Dijk, A. I., Leuning, R., and Guerschman, J. P.: Global vegetation gross primary production
945 estimation using satellite-derived light-use efficiency and canopy conductance, Remote Sensing of
946 Environment, 163, 206-216, 2015.

947 Zhang, Y., Peña-Arancibia, J. L., McVicar, T. R., Chiew, F. H., Vaze, J., Liu, C., Lu, X., Zheng, H., Wang, Y.,
948 and Liu, Y. Y.: Multi-decadal trends in global terrestrial evapotranspiration and its components, Scientific
949 reports, 6, 19124, 2016.